

**Tracing the optimal power flow solutions
via continuation method**

by

Nirlesh Jain

A Thesis Submitted to the
Graduate Faculty in Partial Fulfillment of the
Requirements for the Degree of
MASTER OF SCIENCE

Department: Electrical Engineering and Computer Engineering
Major: Electrical Engineering

Signatures have been redacted for privacy

**Iowa State University
Ames, Iowa**

1993

TABLE OF CONTENTS

1. INTRODUCTION	1
1.1 Introduction	1
1.2 Literature Review	2
1.3 Scope and Objective	4
1.4 Thesis Outline	6
2. VOLTAGE INSTABILITY AND CONTINUATION POWER FLOW	7
2.1 Introduction	7
2.2 Voltage Collapse Phenomenon	7
2.3 Analysis of Voltage Collapse	9
2.4 Continuation Power Flow	10
2.4.1 Introduction	10
2.4.2 Continuation power flow formulation	11
2.5 Voltage Control and Reactive Support	17
2.5.1 Types of reactive sources	17
2.5.2 Reactive power supply and voltage control	20
2.5.3 Effect of reactive power injection on real power transfer capability	21
3. OPTIMIZATION TECHNIQUES	24
3.1 Introduction	24
3.2 OPF Problem Description and Formulation	24
3.2.1 Parametric inequality constraints	25
3.2.2 Functional inequality constraints	26
3.3 Techniques used to Solve OPF Problem	27
3.3.1 Linear programming	28
3.3.2 Newton method	29
3.3.3 Generalized reduced gradient method	32
4. OPTIMAL CONTINUATION POWER FLOW	36
4.1 Introduction	36
4.2 OCPF Algorithm	37

4.2.1	Overview of the OCPF algorithm	37
4.2.2	Problem statement for the optimization	37
4.2.3	Overall solution approach	38
4.3	Features of the OCPF Algorithm	43
4.4	Advantages of the Proposed Algorithm	44
5.	NUMERICAL RESULTS	45
5.1	Introduction	45
5.2	Test Systems and Results	45
6.	CONCLUSIONS AND SUGGESTIONS FOR FUTURE WORK	63
6.1	Conclusions	63
6.2	Suggestions for Future Work	64
	BIBLIOGRAPHY	67
	ACKNOWLEDGEMENTS	73
	APPENDIX A. FORMULATION OF POWER FLOW EQUATIONS IN CPF	74
	APPENDIX B. GRADIENT BASED OPF FORMULATION	76

LIST OF FIGURES

Figure 2.1:	PV curve	10
Figure 2.2:	Illustration of predictor corrector scheme	14
Figure 2.3:	Illustration of CPF via predictor corrector scheme	16
Figure 2.4:	Illustration of shift of critical point with reactive power injection	22
Figure 4.1:	An overview of the OCPF algorithm	38
Figure 4.2:	Detailed block diagram of the OCPF	41
Figure 4.3	Block A	42
Figure 4.4	Block B	42
Figure 5.1:	30-bus New England test system	47
Figure 5.2:	Comparison of the cost for the CPF and the OCPF for 30 bus test system	48
Figure 5.3:	Pgen versus the total load for the 30-bus system for the CPF	48
Figure 5.4:	Pgen versus the total load for the 30-bus system for the OCPF	49
Figure 5.5:	Comparison of the voltage at bus 24 for the CPF and the OCPF in 30-bus test system	51
Figure 5.6:	Comparison of the cost for the CPF and the CAPOCPF for 30-bus test system	52
Figure 5.7:	Comparison of the voltage at bus 24 for the CPF and the CAPOCPF in 30-bus test system	52
Figure 5.8:	Comparison of the voltage at bus 24 for the CPF and the CAPOCPF in 30-bus test system with shunt reactors injected at the same load level	53
Figure 5.9:	Comparison of the reactive losses for the CPF, OCPF, and CAPOCPF in 30-bus test system	53
Figure 5.10:	Comparison of the cost for the CPF and the OCPF for 162-reduced Iowa system	54
Figure 5.11:	Comparison of the voltage at bus 61 for the CPF and the OCPF in 162-bus system	55
Figure 5.12:	Comparison of the cost for the CPF and the CAPOCPF for 162-bus system	56

Figure 5.13:	Comparison of the voltage at bus 61 for the CPF and the CAPOCPF in 162-bus system	57
Figure 5.14:	Comparison of the reactive losses for the CPF, OCPF, and CAPOCPF in 162-bus test system	57
Figure 5.15:	Comparison of the cost for the CPF and the OCPF for 1500-bus system	59
Figure 5.16:	Comparison of the voltage at bus 409 for the CPF and the OCPF in 1500-bus test system	59
Figure 5.17:	Comparison of the cost for the CPF and the CAPOCPF for 1500-bus system	60
Figure 5.18:	Comparison of the voltage at bus 409 for the CPF and the CAPOCPF in 1500-bus system	61
Figure 5.19:	Comparison of the reactive losses for the CPF, OCPF, and CAPOCPF in 1500-bus test system	61

LIST OF TABLES

Table 5.1:	Cost coefficients data for the 30-bus test system	46
Table 5.2:	The CPF and the OCPF results for the 30-bus test system	51
Table 5.3:	The CPF and the OCPF results for the 162-bus test system	58
Table 5.4:	The CPF and the OCPF results for the 1500-bus test system	62
Table 5.5:	Values of reactive sources installed at load buses	62
Table 5.6:	Compares the execution time for the CPF, OCPF, and CAPOCPF	62

1. INTRODUCTION

In the '90s, the electric utility industry has changed greatly in its mode of operation. These changes are:

- **Shift in generation pattern:** Since the 1973 oil embargo there has been a shift in the pattern of generation from oil fired located near the loading site to hydro, mine mouth coal, and nuclear plants located at long distances. There has been a lack of subsequent growth in transmission facilities, due to constraints in acquiring right-of-way from land owners and heightened environmental constraints, leading to loss of congruency between generation and transmission facilities.
- **Non-utility generation:** Significant changes in regulatory philosophy in the electric utility industry has led to non-utility generation, over which operating utilities have little or no control.
- **Open access transmission:** Owners are now required to sell transmission service to any organization requesting it for the purpose of energy transaction as long as capacity is available.

Further recent growth of the industry and an increase in society's dependency on electricity have caused a moderate increase in demand for electric energy.

Such changes have resulted in a highly interconnected and heavily loaded power system network operating closer to limit conditions. There have been increased problems associated with maintaining an acceptable voltage profile and an increase in incidents of voltage instability in bulk power electric

energy systems. Voltage instability is often described as a problem caused by an operating system that exceeds the power limit and involves dynamic as well as static phenomena. Steady state voltage instability occurs as a result of a small disturbance, generally an increase of load or a loss of generation. The disturbance leads to declining of voltages at certain buses. Under these conditions, the operator equipped with automatic control may fail to maintain the voltages. The system then undergoes the state of voltage instability, leading to local or global blackout. The relationship between the loss of this steady state stability and singularity of power flow Jacobian has been observed and presented [1, 5, 16]. The Newton method of power flow solution near this voltage instability point is ill conditioned because of singularity of Jacobian.

1.2 Literature Review

In the past two decades, extensive research has been done in the area of voltage instability. Significant research efforts are underway in an effort to understand the phenomenon, and to develop tools to estimate and avoid voltage collapse. Numerous articles have been published and workshops have been conducted to discuss and solve the voltage instability problem.

A major difficulty encountered in such research is that the Jacobian of Newton power flow equations becomes singular at the steady state voltage instability point. The relationship between loss of this stability and singularity of Jacobian has been shown [1, 2]. Tamura et al. [4] related the voltage instability phenomenon to multiple power flow solutions. As a consequence of the singularity of Jacobian, attempts to find power flow solutions near the critical point are prone to divergence and error. For this reason, Tamura et al.

[4] used the anti-divergence algorithm in an attempt to overcome the numerical divergence. Alvarado et al. [2] and Ajarapu et al. [5] proposed a direct method to detect the voltage instability point, but the method requires a close guess of the critical point. Based on the locally parametrized continuation technique, Ajarapu [2] and Ajarapu and Christy [10] developed a continuation power flow algorithm to trace the power flow solution curve systematically until critical point is reached. The continuation power flow, obtained by using the augmented Jacobian, avoids the singularity of Jacobian near or at critical point. Various indices have been developed to estimate the distance from the critical point. Tiranuchit and Thomas [6] proposed the minimum singular value of the Jacobian of the descriptor network equations as a voltage security index. Ajarapu and Christy [3] used the available tangent vector in continuation power flow (CPF) to provide an index to estimate the collapse point. Ajarapu and Battula [9] used the tangent vector information in performing sensitivity analysis. Tangent vector that contains the differential changes in bus voltage angles and magnitudes information in response to a differential change in load connectivity is used to locate the weak areas in the system.

To avert voltage collapse, operators are seeking tools that can enhance their understanding of where the system is operating with respect to the point of collapse, as well as how much VAR supply is required and where it should be located to achieve a secure system. To address such needs, based on sensitivity and optimization technique, Ajarapu et al. [11] developed a method to minimize the capacities of reactive power to be installed at load buses, to increase the power transfer limit of the network limited by reactive power.

Energy interchange are on the rise to accomplish bulk power economic transfers. The effect of area interchange on voltage stability has been discussed and presented [15]. Iba et al. [22] applied the homotopy continuation method, similar to the continuation power flow developed at Iowa State University, to detect the critical point. The technique of solving a sequence of equations with diminishing degree of simplification until finally the full equation is solved is called homotopy. A continuation parameter is chosen and used to trace the solution curve without numerical ill-conditioning.

To maintain the load voltages and minimize the cost of generation requires an optimal power flow (OPF) formulation. The method developed by Dommel and Tinney [29], using the gradient-based optimization technique, is a benchmark in the solution of the problem of OPF. Burchett et al. [33] used the linear programming technique to solve the OPF problem. Sun et al. [30] developed OPF by the Newton Raphson method and provided decoupling and sparsity techniques to fasten the OPF problem. In other studies [25, 26, 27] Ponrajah and others used the homotopy-based continuation method to solve the OPF problem.

The above methods provide an OPF solution at a current operating point. This thesis describes a methodology that traces the optimal solution path for a continuous increase in load.

1.3 Scope and Objective

To study and prevent the loss of the steady state stability the electric utility industry needs a tool that can avoid the singularity of Jacobian and systematically estimate the distance from this critical point. A robust and well

conditioned tool, the continuation power flow (CPF), has been developed at Iowa State University. The current CPF has the following features and provides the following informations:

- It avoids ill conditioning by using the well conditioned augmented Jacobian in Newton corrector iterations.
- It employs sparsity and optimized step-length techniques to fasten the procedure of obtaining a series of power flow solutions.
- It provides an index to identify the distance from the critical point.
- It performs sensitivity analysis using the tangent vector information. It lists the generators in order of importance in maintaining stability, as well as the branches and buses that are most sensitive to change in load.
- It provides for the effect of load modelling on voltage stability.

Even though the present version of the CPF has been proven to be a powerful tool for analyzing steady state voltage stability, the CPF requires further improvements. The CPF does not take the economics of generation into account. With the worldwide energy crisis and continuous rise in energy prices, reducing the running charges of electric energy, is as important as maintaining the security and reliability of the system. In the current CPF, load voltages are allowed to fall below acceptable limits. Load voltages must be maintained for satisfactory operation of equipment connected to the system.

The objective of this research is to blend the theory of optimization and continuation technique to develop a tool to provide an optimal solution for a given increase in load. This results in the optimal continuation power flow (OCPF), which has the following features:

- The OCPF provides a continuum of optimal solutions for a continuous increase in load in a given direction.
- The total cost of generation is minimized.
- The load voltages are maintained by controlling generator voltages.
- If the generators fail to maintain load voltages, i.e, the solution is not feasible, the method provides a way to control load bus voltages by injecting reactive power sources at suitable load buses.

1.4 Thesis Outline

In Chapter 2, the basic principles involved in analysis of voltage instability and the concepts behind the continuation power flow are discussed. In Chapter 3, the various classical optimization techniques used in optimizing the power flow solutions are reviewed. The development of optimal continuation power flow, which traces optimal solutions for a continuous increase in load, is described in Chapter 4. In Chapter 5, validity of optimal continuation power flow is tested by applying the method for large scale power system network examples. Chapter 6 contains the conclusions and suggestions for future work.

2. VOLTAGE INSTABILITY AND CONTINUATION POWER FLOW

2.1 Introduction

In a recent Institute of Electrical and Electronics Engineers (IEEE) meeting, the voltage stability working group committee used the following definitions:

"Voltage stability has been defined as the ability of a system to maintain voltage so that when load admittance is increased, load power will increase, and so that both power and voltage are controllable."

"Voltage collapse has been defined as the process by which voltage instability leads to very low voltage profile in a significant part of the system."

"Voltage security is the ability of a system not only to operate stably, but also to remain stable as far as the maintenance of system voltage is concerned following any reasonably credible contingency or adverse system change."

Throughout the research, the problem of voltage stability has been examined from the steady state point of view.

2.2 Voltage Collapse Phenomenon

Steady state voltage collapse occurs as a result of inadequate supply of reactive energy, either globally or locally. If generation facilities are located far from load, a voltage drop occurs along the transmission line. Voltage drop is compensated locally or globally by installation of shunt capacitors, on-load tap changing transformers, static VAR compensators, and generator reactive

sources. Adoption of higher transmission voltages and increases in power factor of large generating units decrease the available reactive energy. Increased loading of transmission lines and recent renewed growth in demand has further resulted in increase of reactive losses.

Voltage support is complicated because of the interaction among various buses. Adjustment of voltage at one bus requires the readjustment of voltage at other buses. The situation is further complicated because of the well-accepted wisdom that reactive power dispatch over long distances is limited by increased reactive losses. So even if there is a sufficient reactive energy source, it is of no use if that source is far from the voltage weak area.

Industrial experience reveals that most voltage collapse incidents have followed major disturbances such as loss of transmission or generation equipment. After primary regulation have acted and after the system has settled down to a lower voltage, two factors generally have been observed to jeopardize the voltage stability:

- Load recovery, because of the nature of induction motors and the action of automatic tap changers to restore the secondary voltages. On the customer end, the motors stall with the drop in voltage, causing the voltage to drop further and other motors to stall in cascade fashion. The on-load tap changer, in an attempt to restore voltages, further increases the voltage dependent load and results in further deterioration of voltage, leading to widespread voltage collapse. This may result in massive loss of motor load. The massive loss of motor load may cause the voltages to recover. Transmission line over current protection may not operate due to the fast

voltage recovery. If the root cause of voltage collapse is not removed, voltage may again collapse as motors are restored to service.

- The restriction of generators reactive support imposed by admissible thermal stresses of the machines. Machines are prevented from sustained reactive overload by protecting devices, such as rotor current and maximum voltage set point of generators.

It has been observed that, in most cases, the system settles down to a new operating equilibrium point. However, in a few extreme cases, such an equilibrium point might not exist. Voltage instability results, in the form of sustained monotonic decrease of the voltages, leading to voltage collapse. The collapse leads to the loss of load and a complete shutdown of the affected area.

2.3 Analysis of Voltage Collapse

Planners and operators, aware of the potential for steady state voltage instability, assess the risk of voltage instability and margins by real power-voltage (PV) or reactive power-voltage (QV) curves. PV or QV curves are generated for increasing transfer or load by running a series of power flow solutions. These curves are used by the operators to obtain transfer limits. Figure 2.1 is typical of the PV curve generated for a system that is stable at moderate loading and close to voltage instability at the higher loading. The point "p" on the curve corresponds to the saddle node bifurcation point, i.e, the voltage collapse point. The convergence of power flow solution by Newton method at or near the critical point is ill conditioned because of the singularity of Jacobian. The continuation power flow developed at Iowa State University

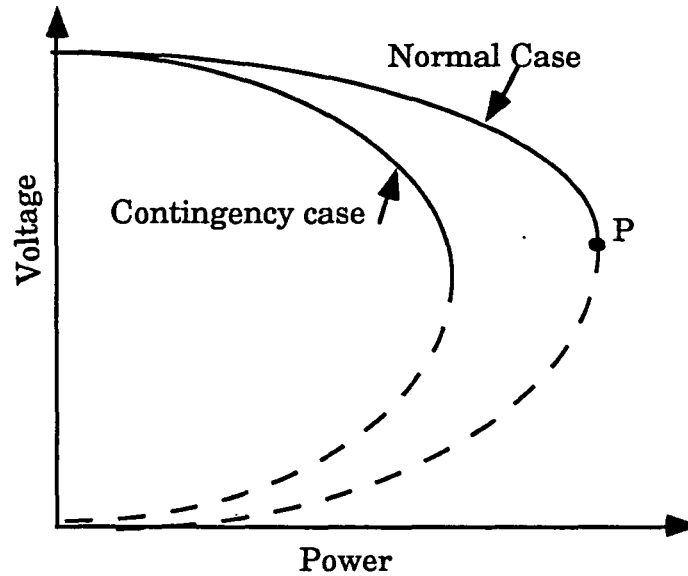


Figure 2.1: PV curve

avoids the ill conditioning by using augmented Jacobian, and in a single run obtains the series of continuum solution for increased transfer or load until a critical point is reached. A brief description of the continuation power flow, which can be used to analyze the steady state voltage stability, is described in the following section.

2.4 Continuation Power Flow

2.4.1 Introduction

Consider a set of nonlinear algebraic equations given by:

$$G(x, \mu) = 0 \quad (2.1)$$

x , G are vectors with n components and μ is a control parameter. It is intended to study how the solutions x of Equation 2.1 vary with μ . For the nonlinear algebraic equation 2.1, more than one zero point may exist for a given fixed

value of the parameter. It has been observed in physical systems that the stationary points are smooth functions of μ except at some exceptional points. This smooth solution set forms the branches of solutions in \mathfrak{R}^{n+1} . If an initial point (x_0, μ_0) is known then a path following method is an algorithm procedure for tracing out these paths.

To be a useful tool, an algorithm has to trace the paths efficiently; it must also be able to recognize the existence of exceptional points to compute them accurately. Continuation methods and homotopy based methods have been introduced and applied to various engineering and scientific applications including applications in civil engineering, chemical engineering and flow research. These techniques provide a systematic approach to trace the branch of equilibrium points.

2.4.2 Continuation power flow formulation

The continuation power flow (CPF) developed at Iowa State University is based on this locally parametrized continuation technique and employs a predictor corrector scheme to trace the solution path of power flow equations.

In order to apply the locally parametrized continuation technique, the power flow equations are reformulated by including a load parameter μ (Appendix B). Reformulated power flow equations can be represented in a general form as

$$G(x, \mu) = 0 \tag{2.2}$$

Here $x = [\delta, v]^T$, where δ represents the vector of bus voltage angles, v is the vector of load bus voltages and μ is the load parameter.

Once a base solution (x_0, μ_0) is obtained corresponding to $\mu = 0$, the continuation problem is to calculate further solutions:

$$(x_1, \mu_1), (x_2, \mu_2), (x_3, \mu_3), \dots,$$

until the critical point corresponding to voltage instability is reached. The mathematical basis of the path following method (or continuation method) is the implicit theorem, which ensures the existence of a smooth path of solutions near (x_0, μ_0) provided $G_\mu(x_0, \mu_0)$ is non-singular. The following section explains how the solution path is traced up to and beyond the critical point (where $G_\mu(x_0, \mu_0)$ is singular) via continuation techniques.

Various continuation techniques that have been developed differ in the type of predictor, parametrization strategy, corrector, and step length control used. The i th continuation step starts from an approximation of (x_i, μ_i) and attempts to calculate the next solution. With predictor-corrector type continuation, the step $i \rightarrow i+1$ is split into two parts. In the first part, the next solution is predicted; in the second part, the predicted solution is corrected to the required solution.

$$\text{Predictor: } (x_i, \mu_i) \rightarrow (\overline{x_{i+1}}, \overline{\mu_{i+1}})$$

(x_i, μ_i) is the power flow solution at base load and $(\overline{x_{i+1}}, \overline{\mu_{i+1}})$ is the predicted solution at increased load level.

$$\text{Corrector: } (\overline{x_{i+1}}, \overline{\mu_{i+1}}) \rightarrow (x_{i+1}, \mu_{i+1})$$

(x_{i+1}, μ_{i+1}) is the corrected solution at increased load level. The predictor-corrector procedure is illustrated in Figure 2.2.

Predictor process: Either the tangent vector or the polynomial extrapolation technique can be used to predict the solution. In the CPF, the next solution is predicted in the direction of the tangent vector, because of the additional information the tangent vector provides. The tangent vector can be used to obtain an index to estimate the distance to critical point from base solution. The tangent vector has also been used to obtain the sensitivity information in the CPF [9, 11].

Thus, the first task in the predictor process is to calculate the tangent vector. The tangent vector is obtained by taking the derivative of Equation 2.2:

$$dG = \frac{\partial G}{\partial \delta} d\delta + \frac{\partial G}{\partial v} dv + \frac{\partial G}{\partial \mu} d\mu \quad (2.3)$$

The factorization of Equation 2.3 results in

$$[G_\delta \ G_v \ G_\mu] \begin{bmatrix} d\delta \\ dv \\ d\mu \end{bmatrix} = 0$$

$[G_\delta \ G_v \ G_\mu]$ is the conventional power flow Jacobian augmented by one column (G_μ) and $t = [d\delta \ dv \ d\mu]^T$ is the tangent vector to be sought. A normalization is imposed in order to give t a unique non-zero length:

$$e_k t_k = 1$$

where e_k is an appropriately dimensioned row vector with all elements equal to zero except k th, which equals one. Proper choice of k guarantees the non-singularity of augmented Jacobian. Thus the tangent vector is obtained by determining the solution of the following equation.

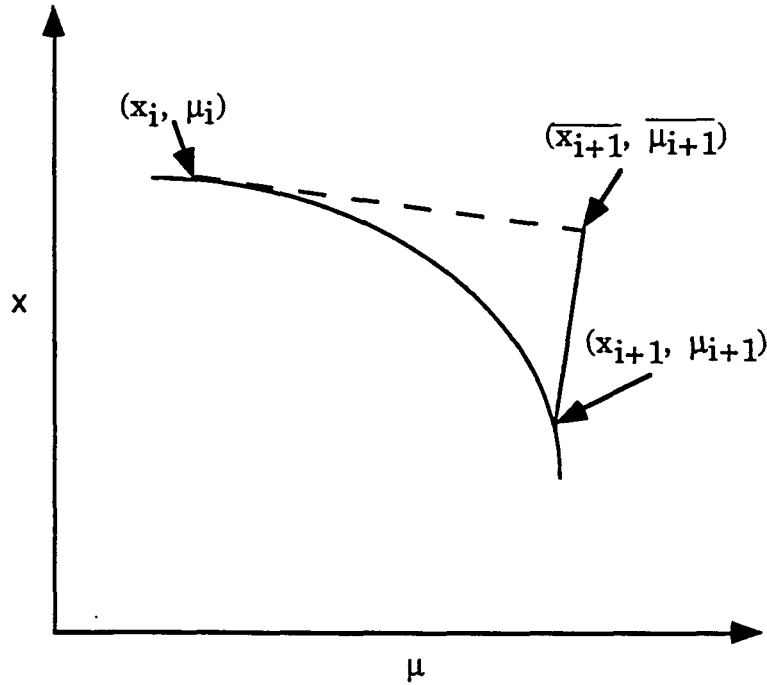


Figure 2.2: Illustration of predictor corrector scheme

$$\begin{bmatrix} G_{\delta} & G_v & G_{\mu} \\ e_k \end{bmatrix} \begin{bmatrix} t \end{bmatrix} = \begin{bmatrix} 0 \\ \pm 1 \end{bmatrix}$$

Once the tangent vector is obtained, the next solution is estimated as

$$\begin{bmatrix} \delta^* \\ v^* \\ \mu^* \end{bmatrix} = \begin{bmatrix} \delta \\ v \\ \mu \end{bmatrix} + \sigma \times \begin{bmatrix} d\delta \\ dv \\ d\mu \end{bmatrix}$$

where '*' denotes the predicted solution and σ is a scalar that designates the step size. The step size is optimally chosen to prevent the corrector iterations from being costly. Various techniques have been used in determining the step

length in the CPF based on sensitivity, radius of curvature, and the continuation parameter.

After the prediction is made, the next step is to correct the predicted solution in the corrector process.

Corrector process: The corrector process depends upon the type of parametrization used. A parametrization is a mathematical way of identifying each solution on the branch. The CPF uses local parametrization, i.e, the original set of equations is augmented by one equation specifying the value of one of the state variables. The new set of reformulating power flow equations is given by

$$\begin{bmatrix} G(x) \\ x_k - \eta \end{bmatrix} = \begin{bmatrix} 0 \end{bmatrix}, \quad x = \begin{bmatrix} \delta \\ v \\ \mu \end{bmatrix}$$

where $G(x)$ denotes the original set of power flow equations and k is the index of the continuation parameter. Once a suitable index k and value of η are chosen, a slightly modified Newton power flow method (altered only in that one additional equation and one additional state variable are involved) can be used to solve the set of equations. This provides the corrector, needed to modify the predicted solution found in the previous section. The critical point corresponds to the point at which maximum loading (and hence maximum μ) occurs. For this reason, the critical point is identified as the point at which the component of the tangent vector corresponding to μ (that is, $d\mu$) is zero, and becomes negative once it passes the critical point. The predictor-corrector process is continuously repeated until the critical point corresponding to voltage collapse is obtained. The CPF process is demonstrated pictorially in Figure 2.3.

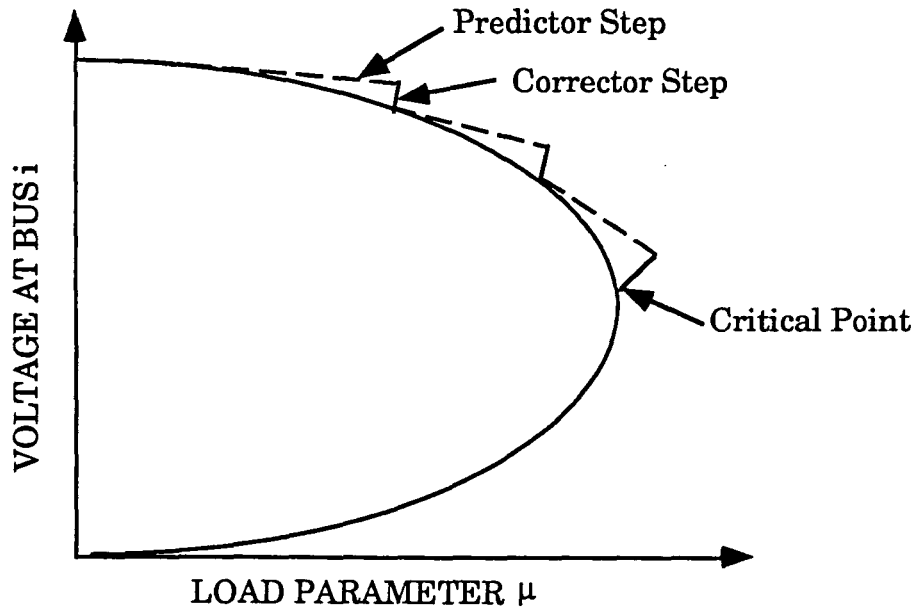


Figure 2.3: Illustration of CPF via predictor corrector scheme

This is the basic continuation power-flow algorithm; details can be found in [2, 3, 12]. In the basic CPF algorithm, the load at each bus is independent of voltage (constant power load model). Christy and Battula [12, 14] in their thesis work included non-linear models in the CPF. Non-linear models represent the actual load on the system as it considers the response of a load change to a change in voltage magnitude. In the basic CPF, the load is increased in steps, corresponding to a change in the continuation parameter and in the specified direction of the load increase.

$$PL_i = PL_{i0} (1 + \mu * pmult_i)$$

$$QL_i = QL_{i0} (1 + \mu * qmult_i)$$

Generation is increased in an arbitrary fashion. For example, the load is distributed according to the original base generation as follows:

$$PG_i = \frac{PG_{i0} * (\text{total change in load})}{(\text{total original base generation})}$$

where PL_{i0} and QL_{i0} are the original active and reactive load at bus i , PG_{i0} is the original generation at bus i , μ is the load parameter, and $pmult_i$ and $qmult_i$ are vectors that designate the direction and the amount of increase.

The main aim of the basic continuation power flow described in the previous paragraphs is to trace the solution path of the power flow equations up to and beyond the critical point. In the basic CPF, the load bus voltages are not maintained within limits. Improvements in the CPF included the use of the weak bus information to determine the possible remedial action for the load voltages. In Lau's thesis work [13], additional reactive sources were used in an attempt to control the load voltages and increase the power transfer capability. In his work, the reactive power compensation was obtained from shunt reactors and shunt capacitors. However, there are other type of reactive sources that can be used to indirectly control the voltage.

The following section discusses the type of these reactive sources. In addition, the relationship between reactive power injection and power transfer capability is described.

2.5 Voltage Control and Reactive Support

2.5.1 Types of reactive sources

The reactive requirements of a power system network are provided by the available reactive sources, which include:

Synchronous generators: Synchronous generators are a major source of reactive power and are limited by machine design parameters. Generators possess the fast dynamic ability to respond to system disturbances and maintain voltages at the desired level. Control of reactive power of generator is achieved by the adjustment of generator field excitation. In a network, generator outage is considered the most critical contingency in terms of the loss of overall reactive supply and the ability to maintain system voltages at permissible levels.

However, the generator reactive power is limited, for the following reasons:

- One must maintain certain generator reactive power margins so that unused reactive power can respond quickly to increased reactive requirements resulting from sudden disturbances.
- Generator reactive power is limited by design parameters. Even if the generator reactive capability is increased by changing the design parameters, increased reactive capability carries a heavy economic penalty outside the normal design limits.
- The installation of generators is dictated by the system active requirements, and not by the need for reactive support. Large transmission reactive losses are incurred if the reactive power of the generator is used to remedy load voltages at the far end of the network.

As a result, additional reactive sources are needed. Additional reactive sources include:

Synchronous condensers: A synchronous condenser is a synchronous machine used to generate reactive power only. A smooth, automatically controlled output can be obtained for a wide range of values. Synchronous condensers are more expensive and require more maintenance than a shunt capacitor. Synchronous condensers are generally installed only if the additional benefits, such as continuous range of reactive control, absorptive capability, better dynamic response characteristics, and greater overload capability are desired in a particular application.

Shunt Capacitors: Shunt capacitors are the most widely used form of reactive compensation in power system networks. Compensation provided by shunt capacitors is a function of the line voltages, and their effectiveness decreases as system line voltage decreases. Shunt capacitors have no moving parts and are therefore highly reliable. Switching of shunt capacitors, achieved by load-break switches or circuit breakers, can be controlled manually or automatically through some control circuitry. This is the cheapest source of additional reactive power.

Series capacitors: Series capacitors compensate for transmission line inductive reactance, thereby reducing the electrical length of transmission lines, reducing line losses and enhancing system capability. Series capacitors introduce the problem of sub-synchronous resonance in the power system network.

Shunt reactors: Shunt reactors are used in a bulk transmission system as a means of holding down system steady state bus voltage when the system is lightly loaded.

High voltage transmission lines: High voltage transmission lines contribute significantly to the total shunt capacitance of the system. The addition of a new transmission line to a system can help in alleviating low voltage by providing additional reactive compensation. However, the construction of a new line, for this purpose alone, is not justified for economic reasons.

Static var compensator (SVC): SVC provides continuous instantaneous changes in reactive output. SVC can be applied to perform steady state voltage regulation functions. However, because of their relatively high cost, most SVC applications are limited to situations in which quick response or independent phase control is required.

Regulating transformers with under load tap changing capability: The system voltage control capability provided by tap changing is generally deemed necessary and well worth the additional expense in transformer cost. The proper use of the tap-changers in conjunction with other reactive devices provides the system operator with considerable flexibility in maintaining system voltage levels. Tap changing capability can be automatically controlled to respond to a control signal, such as voltage signal from a connecting or nearby bus.

2.5.2 Reactive power supply and voltage control

The load voltages are related to power flow injections by the following equations:

$$0 = P_{Gi} - P_{Li} - P_{Ti}, P_{Ti} = \sum_{j=1}^n V_i V_j Y_{ij} \cos(\delta_i - \delta_j - \theta_{ij})$$

$$0 = Q_{Gi} - Q_{Li} - Q_{Ti}, Q_{Ti} = \sum_{j=1}^n V_i V_j Y_{ij} \sin(\delta_i - \delta_j - \theta_{ij})$$

The nodal difference equation for the bus powers in matrix form can be obtained as

$$\begin{bmatrix} \Delta P \\ \Delta Q \end{bmatrix} = \begin{bmatrix} \partial P / \partial \delta & \partial P / \partial v \\ \partial Q / \partial \delta & \partial Q / \partial v \end{bmatrix} \begin{bmatrix} \Delta \delta \\ \Delta v \end{bmatrix}$$

The relation between the effect of change in voltage at bus i because of a change in reactive power at bus j can be obtained by setting $\Delta P = 0$. This results in

$$\Delta Q = \frac{\partial Q}{\partial \delta} * \left[- \left(\frac{\partial P}{\partial \delta} \right)^{-1} * \frac{\partial P}{\partial v} * \Delta v \right] + \frac{\partial Q}{\partial v} * \Delta v$$

The above information can be used to decide the amount of reactive power required to control load voltages at an operating point. Lau et al. [13] used the sensitivity information available from tangent vector to identify the weak buses that need reactive power support.

2.5.3 Effect of reactive power injection on real power transfer capability

The real power transfer capability of a network increases with reactive power injection. Figure 2.4 illustrates how the change in power factor angle (ϕ) resulting from a capacitive reactive power injection would lead to an increase in real power transfer capability. The critical point shifts along a trajectory as

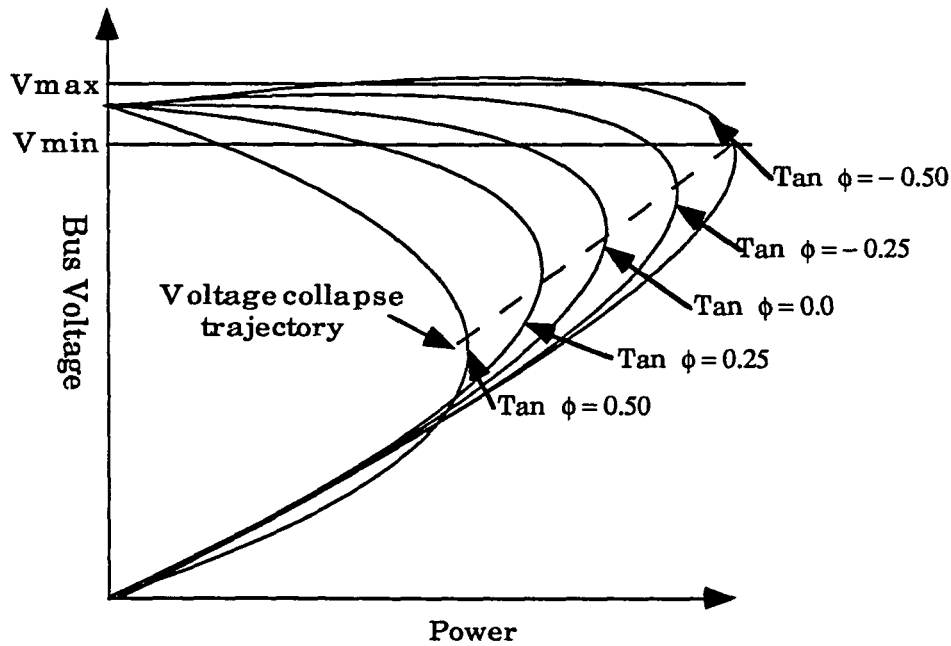


Figure 2.4: Illustration of shift of the critical point with reactive power injection

the injection is increased. Reactive power can be injected in to a power system network up to some maximum value, as the voltage at the bus will cross the V_{max} limit if additional reactive power is injected. It has been observed that highly compensated networks can experience sudden voltage collapses. Indices relying on gradient information for highly compensated systems can be misleading and deceitful.

There is no unique way to improve an operating condition. Some form of compromise is always made in selecting the operating conditions. Our objective in this research is to obtain minimum generation cost with regulated load voltages. To achieve the objective, an optimal power flow (OPF) formulation is required. Various classical optimization techniques that have been applied in the past have been reported in the literature.

The following chapter describes the various approaches to the OPF. In addition, the criteria for the choice of an OPF formulation to be incorporated in optimal continuation power flow (OCPF) are discussed.

3. OPTIMIZATION TECHNIQUES

3.1 Introduction

In this chapter, the optimum power flow (OPF) problem is described and various techniques that are available and used to solve it are discussed. The OPF problem has an objective function and is subject to various constraints.

3.2 OPF Problem Description and Formulation

The purpose of OPF problem is to optimize a performance function while at the same time enforcing the loading limits imposed by the practical system requirements. The performance function is also known as the objective function. In the OPF problem, the most commonly studied objective function is the reduction of the total cost of generation. Other objective functions studied include minimum reactive power generation, maximum loadability, minimum load shedding, minimum losses, and minimum generation emission.

The objective function for the minimization of total cost of generation can be defined as

$$f = \sum K_i (PG_i)$$

where K_i is the production cost for the real power PG_i . Assuming a second order generation cost function, the objective function can be represented as

$$f(x, u) = \sum_{i=1}^{NG} C_{1i} + C_{2i} * PG_i + C_{3i} * (PG_i)^2 \quad (3.1)$$

Here C_i are cost coefficients for unit i .

The real power system requires the optimal solution to satisfy some additional conditions in the form of equality constraints and inequality constraints. An equality constraint forces some specific relationship among the variables to be satisfied exactly. In a power system network, equality constraints are the power balance equation, which requires the net active and reactive power mismatch at each bus to be zero.

$$G(x, u) = 0$$

Here x is a vector of the state variables and u is a vector of the control variables. Inequality constraints impose maximum or minimum limits on the variables or function of variables.

$$h(x, u) \leq 0$$

Inequality constraints can be grouped in two classes:

- (1) Parametric inequality constraints
- (2) Functional inequality constraints

Parametric constraints are the constraints on the control parameters, and functional inequality constraints are the constraints on the dependent variables.

3.2.1 Parametric inequality constraints

Generator real power constraint: The maximum active power generation is limited by thermal considerations and the minimum power generation is limited by the flame instability of the boiler:

$$PG_{\min} < PG_i < PG_{\max}$$

Regulating transformer tap setting: For a two winding transformer, if tappings are provided on the secondary side, the transformer tap setting (t) is limited as

$$t_{\min} \leq t \leq t_{\max}$$

Phase shifter angles: Phase shift angle limit of the phase shifting transformer is given as

$$\Phi_{p\max} \leq \Phi_p \leq \Phi_{p\min}$$

Here Φ_p is the phase shift angle.

Generator voltage: Generator voltages are limited by generator reactive power limits:

$$VG_{\min} < VG_i < VG_{\max}$$

Here VG_i is the generator voltage at PV bus i .

3.2.2 Functional inequality constraints

Reactive power of generator: The maximum reactive power of a generator is limited by overheating of the rotor, and the minimum is limited by the stability limit of the machine.

$$QG_{\min} < QG_i < QG_{\max}$$

Here QG_i is the reactive power generation at generator i .

Transmission line capacity: The flow of active and reactive power through the transmission line circuit is limited by the thermal capability of the circuit.

$$C_i < C_{i\max}$$

Here C_i is current loading at line i , and $C_{i\max}$ is the maximum loading capacity of line i . However, in a voltage constrained power system network, power transfer on transmission lines may be limited by voltage stability limits rather than by thermal limits.

Voltage of load buses: It is essential that the voltage magnitude vary within certain limits at various load buses for the satisfactory functioning of equipment connected to the load buses.

Bus angle: Higher limit is imposed on angles at all buses for reasons of transient stability.

3.3 Techniques used to Solve OPF Problem

The OPF problem has been observed to be characterized by:

- Large dimensionality (thousands of variables).
- Large number of nonlinear equality constraints in the form of power flow mismatch equations to be satisfied exactly.
- Few inequality constraints that are binding at the optimal solution.
- An objective function that is highly non-linear and non-separable, as the objective function includes losses and the controls include various reactive devices.

The application of optimization to the a.c. power flow problem was first formulated by Carpentier [28] in 1966. Since then, various methods have

emerged to solve the above OPF problem. Among them the linear programming, Newton's method, and the generalized reduced gradient are the predominant methods used in industry. Each of these methods has its own peculiar limitations in term of flexibility, adaptability and performance. It is always difficult to identify the method with the best combination of properties.

3.3.1 Linear programming

In general, the OPF is expressed as a nonlinear optimization problem. The OPF problem is solved using linear programming (LP) techniques by expressing the OPF as a linear optimization problem.

Simply stated, linear programming seeks to find the optimum value of a linear objective function while meeting a set of linear constraints. A non-linear generation cost curve is approximated by a series of piece-wise linear curves. The OPF problem is typically subdivided or decoupled into two separate sub-problems:

- Constrained Economic Dispatch
- Constrained Var Dispatch

In both the constrained economic dispatch and the constrained var dispatch, the objective function and the parametric and functional constraints are linearized by piece-wise curves at the base power flow solution. These curve are solved iteratively by various linear programming approaches such as the primal dual, and the single phase.

The drawbacks of LP technique lie in the requirement that all relations be linear or approximated as linear, and that all variables must not be moved

simultaneously towards the solution point. This technique cannot be used to solve non-separable objective functions efficiently. However, the LP technique can directly enforce the limits on variables and on constrained quantities that are linear functions of the variables. The enforcement of these limits presents difficulties in the classic nonlinear gradient or the Newton techniques. It has been observed that decoupling models are inadequate when voltage-related constraints impose restrictions on MW scheduling and when very high coupling exists in the power system network. The fast solution of the OPF by the linear programming technique using the decoupled version cannot be used in power system networks limited by voltage constraints.

3.3.2 Newton method

In the Newton method, the constrained objective function is changed to the unconstrained form by use of the classical optimization method of Lagrangian multipliers:

$$L(x, u) = f(x, u) + \lambda^T * G(x, u) \quad (3.2)$$

Here $G(x, u)$ is a set of active equalities and λ corresponds to Lagrangian multipliers equal to the number of active equalities. The set of active equalities always includes the power flow equations for scheduled load and generation. It also includes the following sets of binding inequalities:

- The equation of inequality functions constrained at their limits.
- The minimum and maximum variable limits.

The minimum of the objective function is at a point at which partial derivatives obtained with respect to all variables are zero, i.e, Kuhn-Tucker

(K-T) conditions are satisfied as follows:

$$\frac{\partial L}{\partial x} = \frac{\partial f}{\partial x} + \left[\frac{\partial G}{\partial x} \right]^T \lambda = 0 \quad (3.3)$$

$$\frac{\partial L}{\partial u} = \frac{\partial f}{\partial u} + \left[\frac{\partial G}{\partial u} \right]^T \lambda = 0 \quad (3.4)$$

$$\frac{\partial L}{\partial \lambda} = G(x, u) = 0 \quad (3.5)$$

The above equations are non-linear and can only be solved by some iterative method. In the Newton optimal power flow approach, the above non-linear equations are iteratively solved using Newton Raphson iterations. The partial derivatives are obtained for the above equations with respect to all variables and set equal to zero, resulting in the following algebraic form:

$$WX = b \quad (3.6)$$

$$W = \begin{bmatrix} H & -J^T \\ J & 0 \end{bmatrix} \quad (3.7)$$

Here W is the Lagrangian matrix and J is the Jacobian matrix. H is the Hessian matrix, symmetric in nature and consisting of the second partial derivatives of Lagrangian objective function w.r.t to x , u , μ , and λ . X is a vector of unknown variables and b is a vector of mismatch at the approximated value of unknowns. The value of the vector X is calculated by solving the equation 3.6, and then substituting to obtain the updated Lagrangian matrix values and the vector b . This procedure is repeated until the mismatches obtained are zero.

Various techniques have been developed to reduce the time for the above computing process. The techniques include decoupling of the Hessian matrix and the use of sparsity in the highly sparse Hessian and Jacobian matrices.

The set of binding constraints at the optimal point is unknown. The set of binding inequalities used at the start may change as the iterations proceed. The enforcement of different types of inequalities has different effects on the form of the Hessian matrix, the Jacobian matrix and the vector b . Heuristic methods are used to approximately predict the effects from the known behavior of the power system and the solution process. An algorithm that may be used [30] employs a main and a trial iteration approach to solve the K-T equations.

The trial iteration is performed either by partial refactorization or by compensation and is generally used to identify the currently binding inequalities. In each trial, the effects of different combinations of constraint enforcement and release at a tentative solution point are examined. Various heuristic strategies are employed to minimize the number of trial iterations. After the trial iterations, a main iteration is performed. In the main iteration, the decoupled Hessian is fully factorized and the corresponding equations are solved. The procedure is repeated until the K-T conditions are satisfied.

The solution of the OPF problem by Newton's method requires the approximate knowledge of Lagrangian multipliers. Solution of the OPF by Newton's method can suffer from divergence if the point guessed is far from the actual solution point. Identifying the correct binding inequalities is still a challenge in this approach to the OPF and Newton's method still suffers from deficiencies.

3.3.3 Generalized reduced gradient method

In 1968, Dommel and Tinney [29] introduced the reduced gradient approach to the OPF problem. The generalized gradient method of solving the OPF is based on power flow solution by Newton's method, a gradient adjustment algorithm for obtaining the minimum and penalty functions to account for dependent constraints.

In the strict sense, the Lagrange function deals only with equality constraints. Inequality constraints can be incorporated using the "penalty function" approach. The Lagrangian objective function obtained in this case is given by

$$L(\mathbf{x}, \mathbf{u}) = f(\mathbf{x}, \mathbf{u}) + \lambda^T * G(\mathbf{x}, \mathbf{u}) + \text{penalty terms.} \quad (3.8)$$

The Lagrangian multipliers are the same as in Equation 3.2 corresponding to the equality constraints. The penalty term corresponds to functional dependent constraints and are of the form:

$$\begin{aligned} \omega_j &= P_j(x_j - x_{j\max})^2, \text{ whenever } x_j > x_{j\max} \\ \omega_j &= P_j(x_j - x_{j\min})^2, \text{ whenever } x_j < x_{j\min} \end{aligned} \quad (3.9)$$

Here P_j is the penalty constant for j th state variable and ω_j is the penalty function. The penalty function approach forces the solution to obtain an optimal point sufficiently close to constraints. The penalty method seems to have the following advantages for the functional constraints:

- Functional constraints in the OPF generally have soft limits, i.e, the voltages at PQ buses should not exceed 1.0, but 1.01 is still permissible.

- The penalty approach does not increase the computing time.
- The method always yields a feasible solution.

In the penalty method approach, quadratic penalties are used as shown in Equation 3.9. Because the limits on voltage are more severe and more important, they require larger penalties. On the other hand, limits on reactive power generation (QG) can be less rigid, as QG can be expanded by installing reactive or capacitive equipment and, therefore, require smaller penalties. Very large penalty factors corresponding to load voltages will unload the unit, affecting the maximum and reducing the total combined cost. The combined cost is a minimum when all units are operating at an equal incremental combined cost. Finding the stationary point of the Lagrange function has the effect of optimizing the constrained problem. The augmented Lagrangian function is differentiated wrt to x u λ as in Equations 3.3, 3.4, 3.5. These equations are solved by a simple iteration scheme involving gradients, an approach called the steepest descent approach. A gradient of the objective function $f(x, u, \lambda)$ at any point (x, u, λ) is a vector in the direction of the largest local increase in the function. In order to achieve the minimum cost of the objective function, the solution should proceed in the direction opposite to the gradient of $f(x, u, \lambda)$, i.e, the direction of steepest descent. One step in the direction of the steepest descent for optimization does not yield the final minimum. This process is applied repeatedly until the final minimum is reached.

The main steps involved in the gradient method are the following:

- (1) Assume a set of control variables (u).

- (2) Find a feasible power flow solution by Newton's method.
- (3) Once the power flow solution is obtained, Equation 3.3 is solved for λ as follows:

$$\lambda = - \begin{bmatrix} \frac{\partial G}{\partial x} \end{bmatrix}^{-T} \frac{\partial f}{\partial x} \quad (3.9)$$

Here the matrix $\begin{bmatrix} \frac{\partial G}{\partial x} \end{bmatrix}$ is the power flow Jacobian. Detailed formulation in terms of power flow equations can be found in Appendix B. The factored power flow Jacobian is available already from the power flow solution by Newton's method. The calculation of the Lagrangian multipliers amounts to only one more repeat solution of a linear system.

- (4) The Lagrangian multipliers obtained in step 3 are substituted in to Equation 3.4 to compute the gradient. The gradient vector represented by ∇f measures the sensitivity of the objective function wrt to a change in the control parameters.

$$\nabla f = \frac{\partial f}{\partial u} + \begin{bmatrix} \frac{\partial G}{\partial u} \end{bmatrix}^T \lambda \quad (3.10)$$

- (5) If the norm of the gradient vector is small, the minimum has been reached.
- (6) If the norm of the gradient vector is not small, then the control parameters are changed in the direction of the negative gradient vector:

$$[u_{\text{new}}] = [u_{\text{old}}] - c\Delta f$$

where c represents the step size. The choice of the step size is critical. A small value ensures convergence but increases the number of adjustment cycles, and too large a value for c causes oscillations around the minimum. Various methods for selecting the step size can be employed. In one method the objective function is minimized wrt to c in order to move by one step. A fixed variable can also be selected.

The above steps are straightforward and do not pose any computational problems in formulation and computation. Once the new control parameters are obtained, the power flow solution is obtained corresponding to these new control parameters by Newton's method. Drawbacks of this approach include the slow convergence with the steepest descent direction and the ill conditioning resulting from the penalty function. The OPF formulation by this approach can be ill conditioning near the critical point (corresponding to voltage collapse) because of the singularity of the Jacobian. This ill conditioning is avoided in the OCPF approach by using well augmented Jacobian.

In the next chapter the criteria for choosing the OPF technique in the optimal continuation power flow (OCPF) are discussed and the OCPF algorithm is developed.

4. OPTIMAL CONTINUATION POWER FLOW

4.1 Introduction

The optimal continuation power flow (OCPF) method uses the systematic approach of the continuation technique to provide a series of solutions for the increased transfer or load level. It uses the OPF technique to obtain each solution as an optimal point. This results in an algorithm to trace the optima of the equality and inequality constrained optimal power flow as a function of a load parameter. Available optimization techniques are used to find an optimal power solution for a fixed load. It is often necessary to know the effects of a change in load parameter on the optima solution over a wide range. The optimal continuation power flow approach provides a systematic way to trace the optima for a continuous increase in load in the given direction via continuation techniques. This approach also reveals the critical point corresponding to voltage instability.

As a series of optimal solutions are obtained up to the critical point, the optimal power flow solution can be ill conditioning near the critical point. The simplicity of gradient based OPF technique and the use of a well-conditioned augmented Jacobian (obtained in the CPF) in optimal corrector iterations are the main decision factors in choosing the gradient-based OPF technique for development of the OCPF. The following section provides an overview of the OCPF algorithm.

4.2 OCPF Algorithm

4.2.1 Overview of the OCPF algorithm

The OCPF starts at the given base load. An optimal solution is obtained corresponding to this base load using a gradient-based optimization technique. The OCPF mainly consists of the following two parts:

Continuation process: In the continuation process, the next solution is first predicted in the direction of the tangent vector at increased load level. The predicted solution is corrected to the required solution. The output of the continuation process is then fed in to the optimization process.

Optimization process: The corrected solution is iteratively optimized in steps via a gradient-based optimization technique. Once the optimal solution is obtained, the output is fed back in to the continuation process so that the next solution can be predicted.

This procedure continues until a critical point corresponding to voltage collapse is obtained. Figure 4.1 illustrates the overview of the OCPF algorithm.

4.2.2 Problem statement for the optimization

The objective function to be minimized is the same as described in Chapter 3 (Equation 3.1):

$$f(x, u) = \sum_{i=1}^{NG} C_{1i} + C_{2i} * PG_i + C_{3i} * (PG_i)^2$$

The objective function is subjected to the following equality constraints:

$$G(x, u, \mu) = 0$$

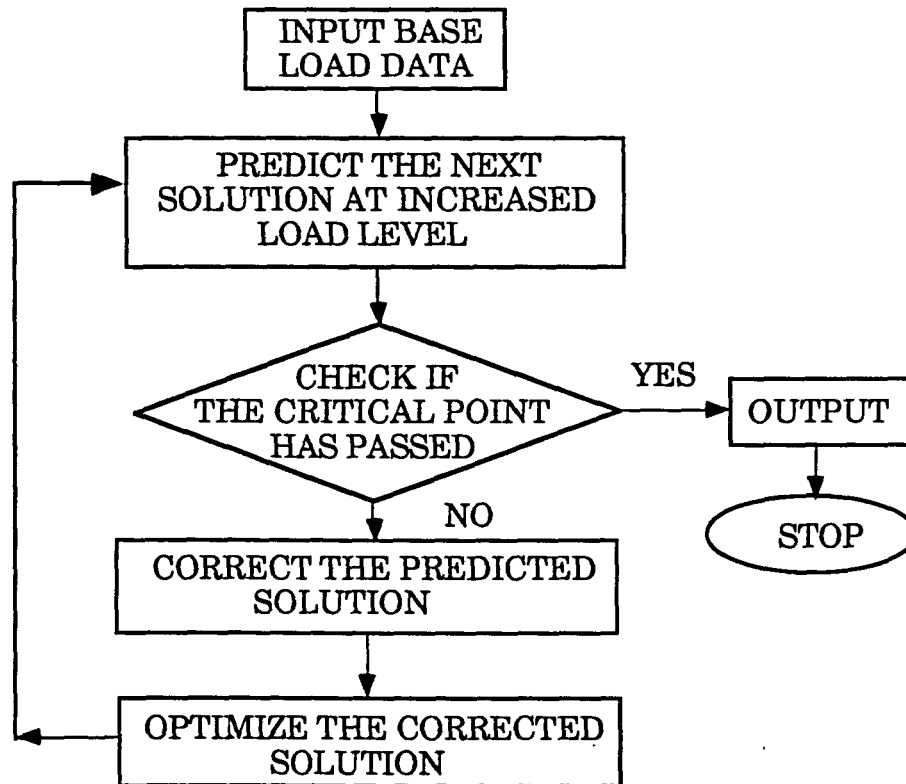


Figure 4.1: An overview of the OCPF algorithm

Here $G(x, u, \mu)$ are the reformulated power flow equations after a load parameter μ has been included. The objective function is also subjected to following inequality constraints:

$$h(x, u, \mu) \leq 0$$

Generator voltages and generator powers are the parameters changed during optimal tracking in the OCPF. The transformer tap setting is not changed.

4.2.3 Overall solution approach

The overall algorithm includes the following steps:

- Step 1** Solve the power flow equations at the base load using Newton Raphson iterations.
- Step 2** Perform optimization at base load.
 - 2.1 Obtain Lagrangian Multipliers using Equation 3.9.
 - 2.2 Substitute the Lagrangian multiplier in Equation 3.10 to obtain the gradient vector. If the norm of the gradient vector is small, go to Step 3; otherwise go to Step 2.3.
 - 2.3 Adjust the control parameters in the negative gradient direction. Return to Step 1.
- Step 3** Select the load parameter as the continuation parameter.
 - 3.1 Solve for the tangent vector. If the tangent vector component corresponding to λ is negative, then stop; the critical point has reached.
- Step 4** Predict the solution in the direction of the tangent vector. This step includes the following sub steps:
 - 4.1 Select the step size.
 - 4.2 Increase the load in the given direction.
 - 4.3 Obtain the total increase in load and distribute the load among the generators in the optimal direction calculated using

$$PGDIF_i = PG_{ia} - PG_{ib}$$

where PG_{ia} = generation after the nth optimal iteration for a particular predictor step and PG_{ib} = generation before the nth optimal iteration for the same predictor step.

$$PG_i = PG_i + \| PGDIF_i \|_1 * \text{total change in load}$$

- 4.5 Change the voltages and angles in the direction of tangent vector.
- Step 5** Solve the Newton power flow equations using the augmented Jacobian to correct the required solution.
 - Step 6** Perform optimization.
 - 6.1 Perform Sub-step 2.1
 - 6.2 Obtain the gradient vector. If the norm of the gradient vector is small, or the number of optimal iterations exceeds the maximum number of iterations, go to Step 7.
 - 6.3 Adjust the control parameters in the negative gradient direction and go to Step 5.
 - Step 7** Check for the load voltage violations. If the load voltages are violated, then reactive sources are installed with capacities calculated as in Section 2.5.2. There are two ways to continue once the value of reactive sources is calculated. Either solve the power flow equations at the current load level or without solving the power flow equations at current load level, predict the next solution. The later approach saves the cpu time while the former is more accurate. These two approaches have been compared for a 30-bus test system and numerical results obtained are presented in Chapter 5.
Go to Step 5. Else go to Step 3.1.

These steps are illustrated with the help of a block diagram in Figure 4.2. Block A and block B are given in Figures 4.3 and 4.4 respectively.

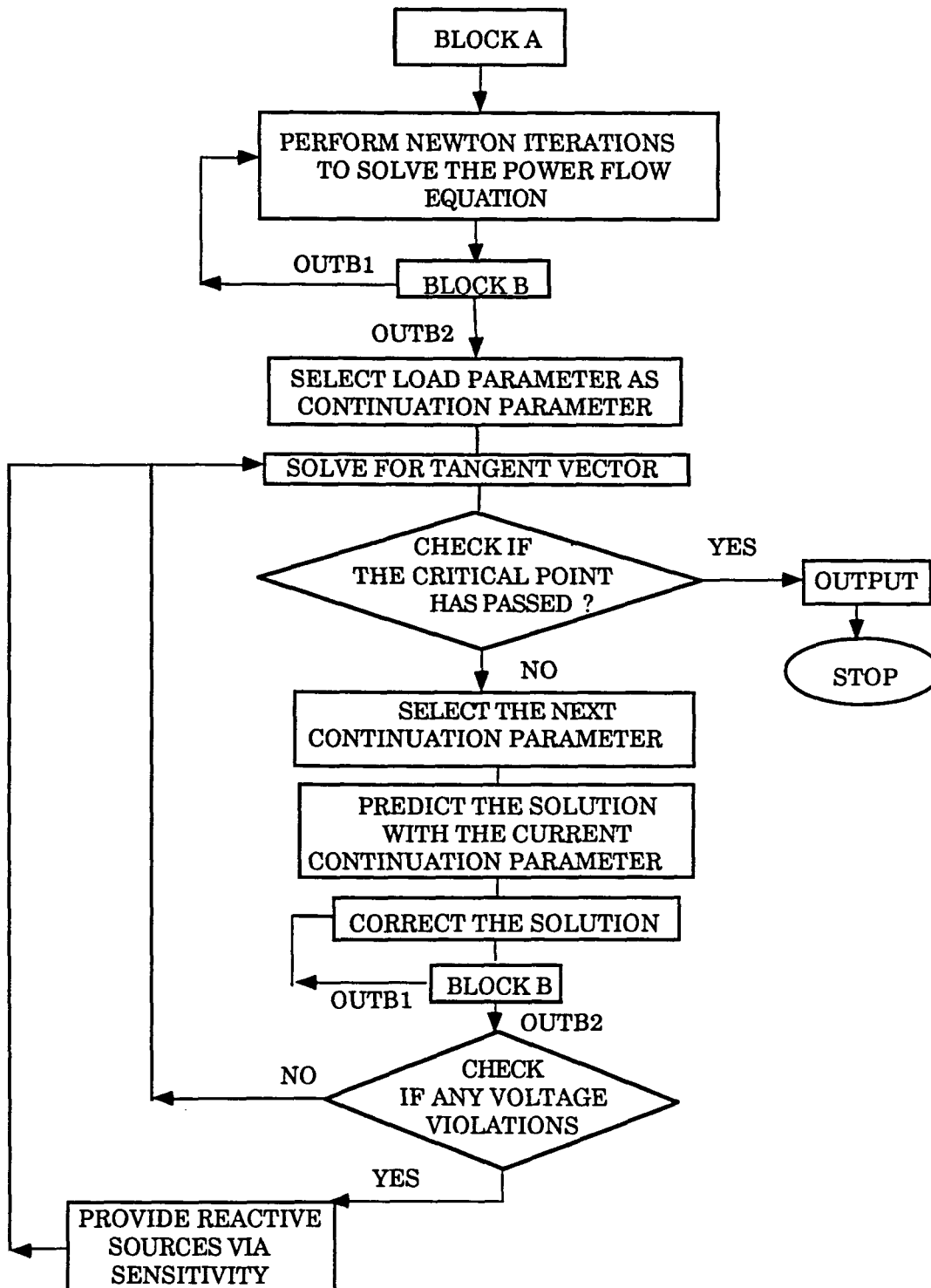


Figure 4.2: Detailed block diagram of the OCPF

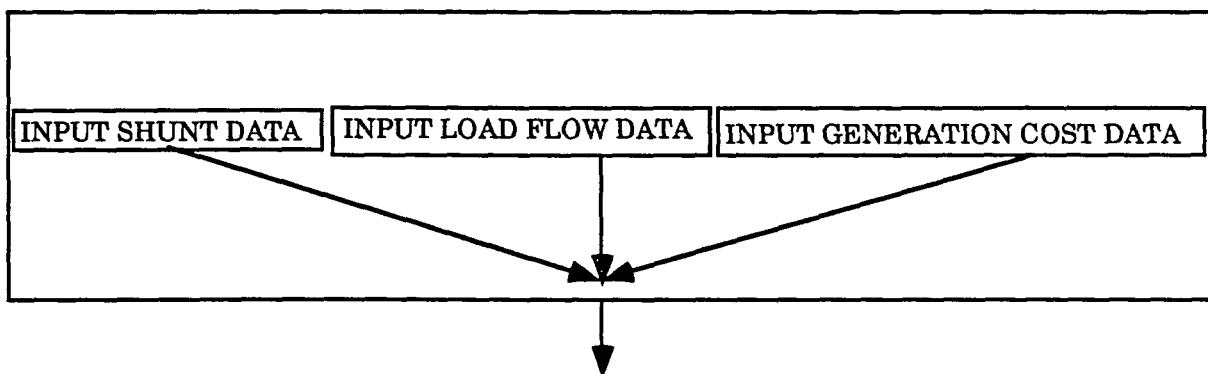


Figure 4.3: Block A

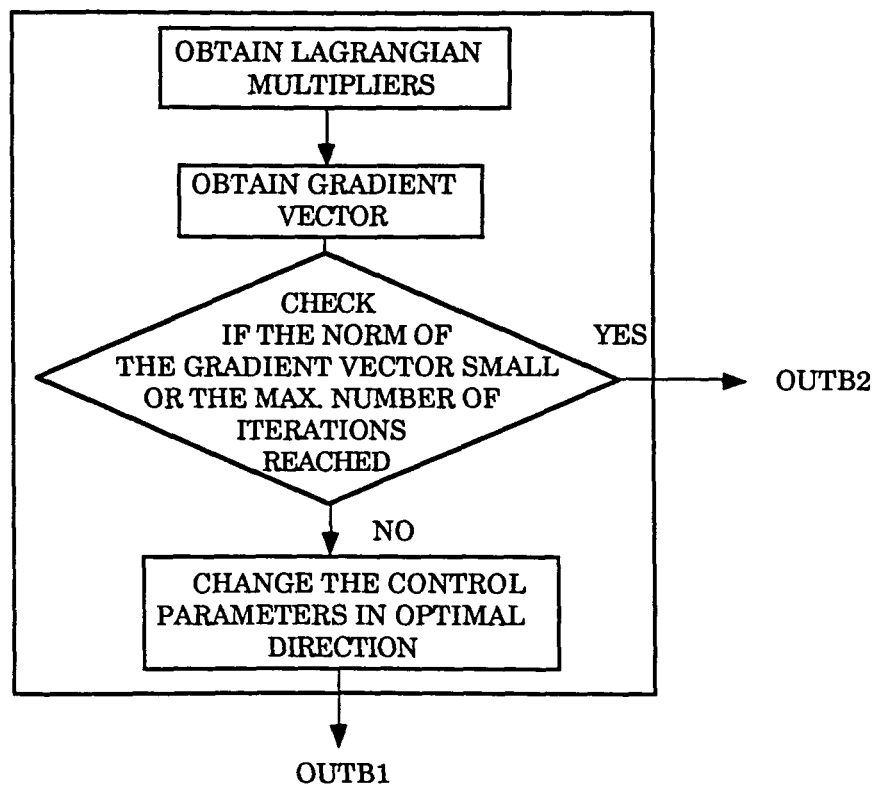


Figure 4.4: Block B

4.3 Features of the OCPF Algorithm

- In the predictor-corrector process, the step size is chosen optimally on the basis of radius of curvature and previous step size. This prevents the the process from being excessively time consuming.
- These Linearized power flow equations at an operating point are solved using a sparsity based algorithm to reduce the execution time, as the Jacobian is highly sparse in nature.
- The Jacobian is not continuously factorized during the Newton iterations. If the dimension of the Jacobian changes because of the change in status of buses from PV to PQ or PQ to PV, then only the Jacobian is updated and factorized in the Newton iterations to solve the power flow equations. This reduces the number of factorizations of the Jacobian, resulting in a saving of CPU time.
- The Lagrangian multipliers require the factorization of a power flow Jacobian matrix. Instead of a power flow Jacobian as used in reference [29], a well-conditioned augmented Jacobian is used. However the validity of using the same augmented Jacobian remains as long as the load parameter is the continuation parameter.

$$\begin{bmatrix} \partial P/\partial \delta & \partial P/\partial v & \partial P/\partial \psi \\ \partial Q/\partial \delta & \partial Q/\partial v & \partial Q/\partial \psi \\ 0 & & 1 \end{bmatrix}^T \times \begin{bmatrix} \lambda_P \\ \lambda_Q \\ \lambda_0 \end{bmatrix} = -Z \begin{bmatrix} \partial P_1/\partial \delta \\ \partial P_1/\partial v \\ 0 \end{bmatrix} - \begin{bmatrix} \Sigma \partial \omega_j(\delta)/\partial \delta \\ \Sigma \partial \omega_j(v)/\partial v \\ 0 \end{bmatrix}$$

The matrix on the left side is the augmented Jacobian.

- In the optimal corrector iterations, the use of well-augmented Jacobian is made.

- Optimal solutions with respect to cost of generation are available for the continuous increase in the load.
- A constant step size is chosen for changing the parameters in the negative gradient direction.
- The algorithm has been applied to systems as large as 1,500 buses and is capable of handling even bigger systems.

4.4 Advantages of the Proposed Algorithm

The advantages of the proposed algorithm include:

- This approach uses the well-conditioned augmented Jacobian to avoid the ill-conditioning resulting in the OPF formulation near the critical point. The ill-conditioning is avoided by using the well-augmented Jacobian in optimal corrector iterations. Even in calculating the Lagrangian multipliers, the same augmented Jacobian is used.
- The proposed algorithm has all the advantages of the gradient approach, which makes the overall algorithm simple. The algorithm always obtains a series of feasible operating points.
- In the proposed approach, the total load added at the predictor step is distributed among the generators in the optimal direction. This reduces the number of iterations needed for optimizing the solution, which results in a saving of execution time.

In the next chapter, the OCPF algorithm is applied to real power system networks, and the results obtained are discussed.

5. NUMERICAL RESULTS

5.1 Introduction

Three power system networks are used to test the validity of the OCPF algorithm as explained in Chapter 5. The system networks used are real and reasonably sized. Because of the unavailability of cost coefficients for the generators, fictitious data have been used for economic modeling.

5.2 Test Systems and Results

IEEE New England test system: In this system that is commonly used in voltage stability research, there are a total of 9 generators and 20 PQ buses. Bus 30 is the slack bus. Table 5.1 gives the cost coefficients that are used in modeling generators cost. The system is shown in Figure 5.1.

Figure 5.2 compares the cost of generation for the CPF and the OCPF (without shunt reactive power injection) for a continuous increase in load. It is observed that, during optimal tracking, the total cost decreases greatly during the first few steps and then decreases only slightly and even increases later on. The cost of generation is always lower for the OCPF than for the CPF.

Figure 5.3 and Figure 5.4 plots the generator bus and slack bus real power generation levels for the CPF and the OCPF (without shunt reactive power injection) respectively. Figure 5.3 illustrates how the generation is increased in the basic CPF; the generation increase is along straight lines, with the slope higher for the higher base generation. Figure 5.4 illustrates the generation increase in the OCPF (without shunt reactive power injection); the

generation increase in the OCPF corresponding to an increase in load that is not along straight lines. Figure 5.4 shows that generator 6 with the minimum generation cost (seen from Table 5.1) has the highest generation level. The change in the slack bus generation level in the OCPF run is large as compared to the CPF.

Table 5.1: Cost coefficient data for the 30-bus test system

units	coefficient C1i	coefficient C2i	coefficient C3i
2	59.0	340.0	41.0
6	39.0	300.0	32.0
10	39.0	312.0	48.0
19	49.0	382.0	63.0
20	58.0	356.0	48.0
22	40.0	300.0	43.0
23	58.0	345.0	47.0
25	38.0	304.0	42.0
29	58.0	360.0	58.0
30	55.0	351.0	45.0

Figure 5.5 compares the voltage profile for a bus for the CPF and the OCPF (without shunt reactive power injection). Bus 24 is observed to be the most critical bus (maximum drop in voltage magnitude corresponding to the change in loading parameter μ) during the CPF run according to information

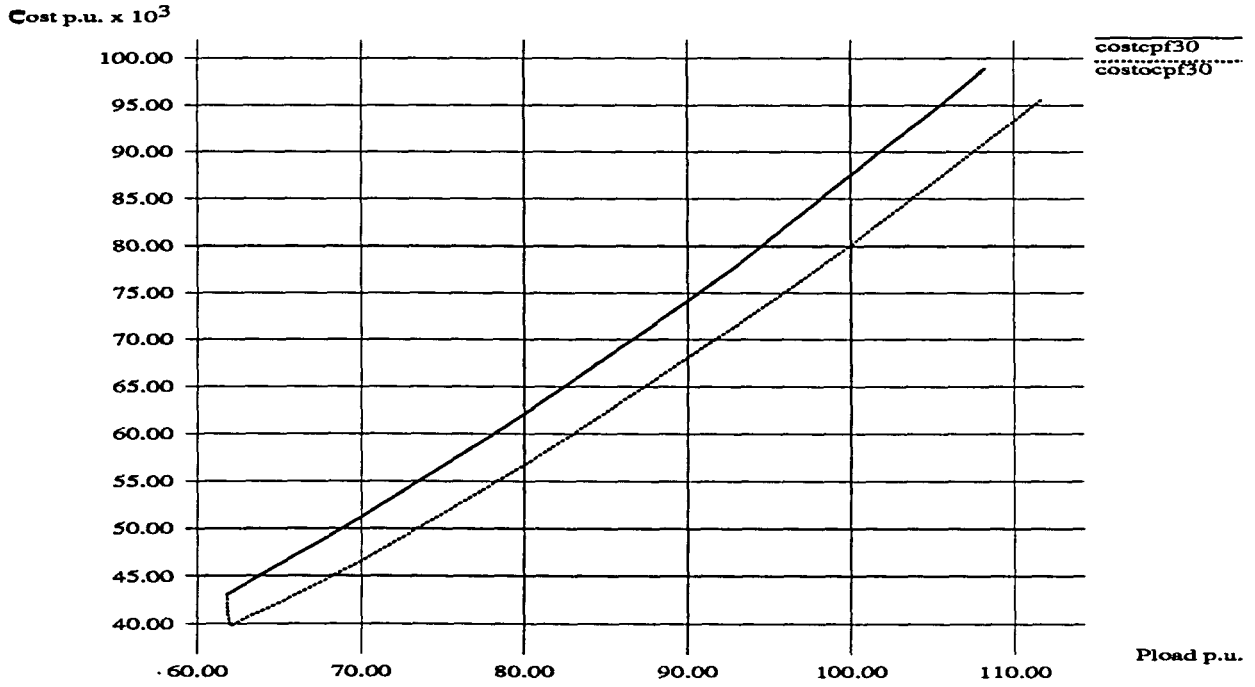


Figure 5.2: Comparison of the cost for the CPF and the OCPF for 30-bus test system

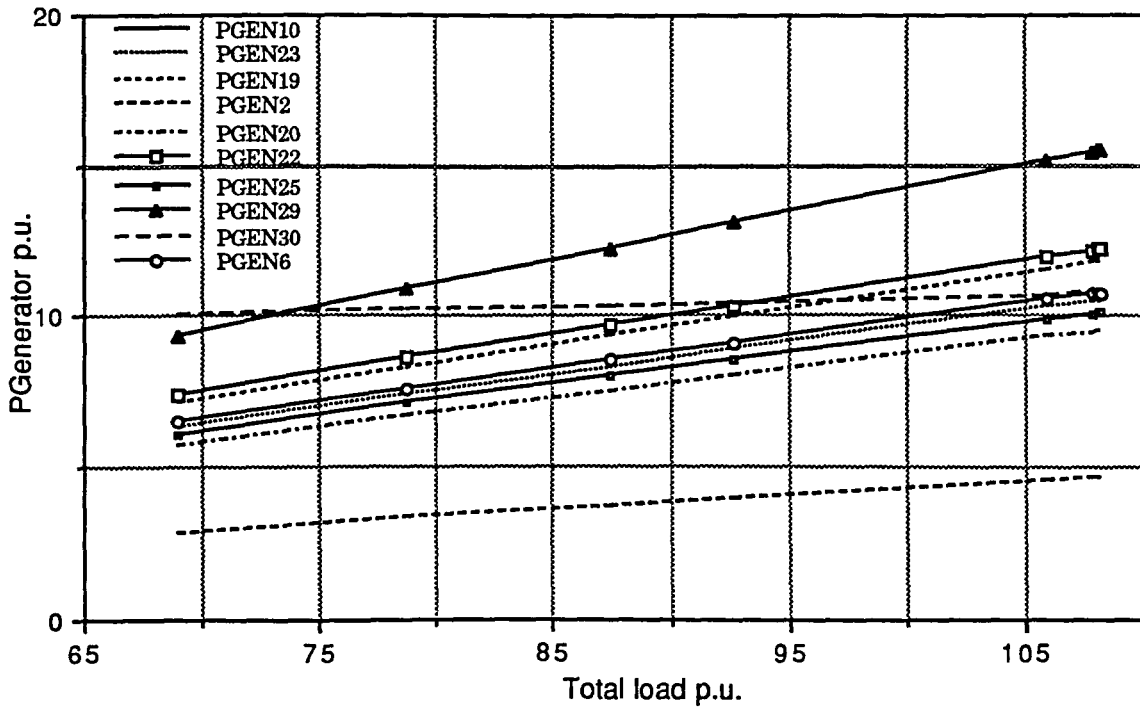


Figure 5.3: Pgen versus the total load for 30-bus system for the CPF

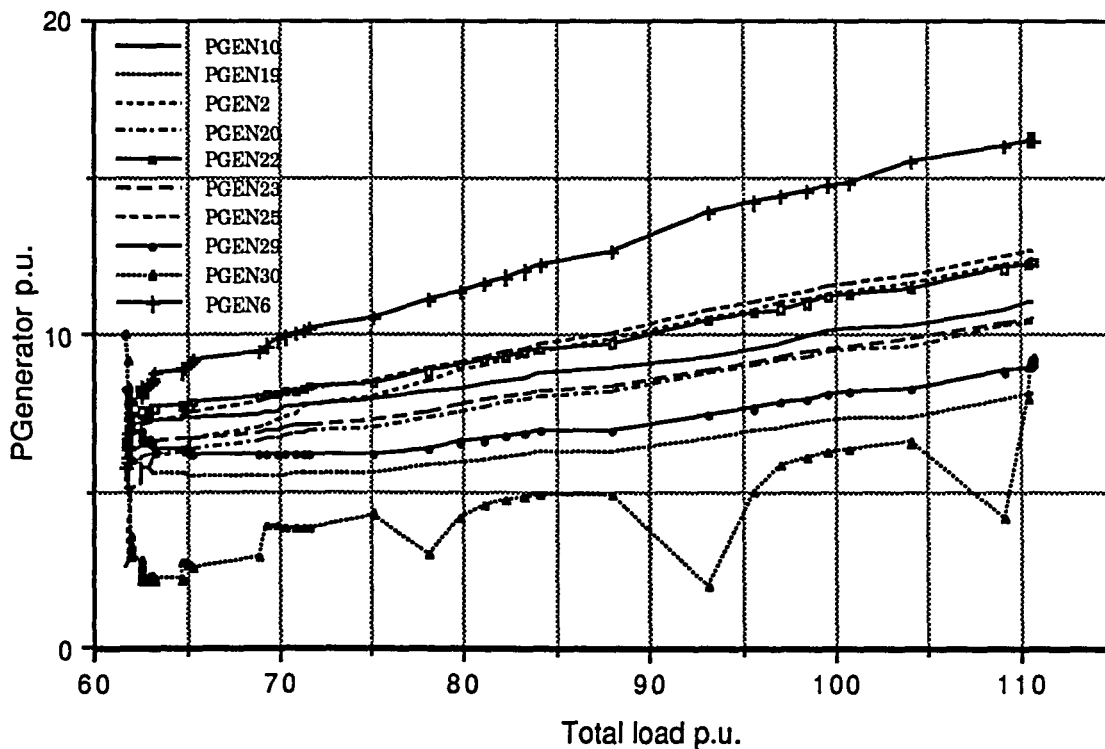


Figure 5.4: Pgen versus the total load for the 30-bus system for the OCPF

obtained via the tangent vector. This bus seemed to be most suitable for comparison of voltage profile for the CPF and the OCPF. At a load value of approximately 9,500 MW, the OCPF boosts the voltage at bus 24. This boost may be because of the voltage interaction between different buses. The voltage magnitude at one bus may affect the voltage magnitude at other buses. The CPF as well as the OCPF curves have been traced in this Figure up to the critical point. However, in actual operating conditions, once the load voltages fall below acceptable limits, load voltages have to be regulated. If system conditions have reached the point at which voltage regulation is not feasible, further increase in the transfer of power is not allowed. Figure 5.5 shows the voltage boost obtained at various loading points during optimal tracking in the

OCPF. If 0.95 p.u. is considered to be the minimum acceptable limit for the load voltages, then in the CPF total load transfer capability of the system is 10,800 MW, and in the OCPF it is 11,080 MW. The transfer capability of network increases by approximately 280 MW with the OCPF. This increase in MW is because of the increased generator voltage magnitude during optimal tracking, which results in a better load voltage profile.

Figure 5.6 compares the cost of generation for the CPF and the OCPF (with shunt reactive power injection). The costs of the reactive sources is not included in the graphs. The CAPOCPF represents the OCPF with shunt reactive power injection. Figure 5.7 compares the voltage profile for the CPF and the CAPOCPF. It illustrates how the voltage is boosted via reactive sources when the load level is at a value of approximately 11,300 MW. In Figure 5.7 after the values of shunt reactors is calculated in CAPOCPF, the next solution is predicted without updating the voltages and the Jacobian. Figure 5.8 plots the voltage levels for the CPF and the CAPOCPF for the case; where the Jacobian and the load voltages are updated after the values of shunt reactors is obtained by performing Newton iterations, at the same load level in the CAPOCPF. Results obtained with updating at the same load level are more accurate. However, updating increases the computing time. Figure 5.7 illustrates the increase in transfer capability of the network via shunt reactive power injection by 2,020 MW. This increase results from the local reactive load being now supplied by the shunt reactive sources installed at the load buses. This results in decreased effective reactive load and also reduced reactive losses. Figure 5.9 plots the reactive losses for the CPF, OCPF, and CAPOCPF. Table 5.2 gives the transfer capability information for the CPF, OCPF, and CAPOCPF.

Table 5.2: The CPF and the OCPF results for the 30-bus system

Method	Maximum system real power transfer in p.u.
CPF	108.0
OCPF without reactive power injection	110.8
OCPF with reactive power injection	128.2

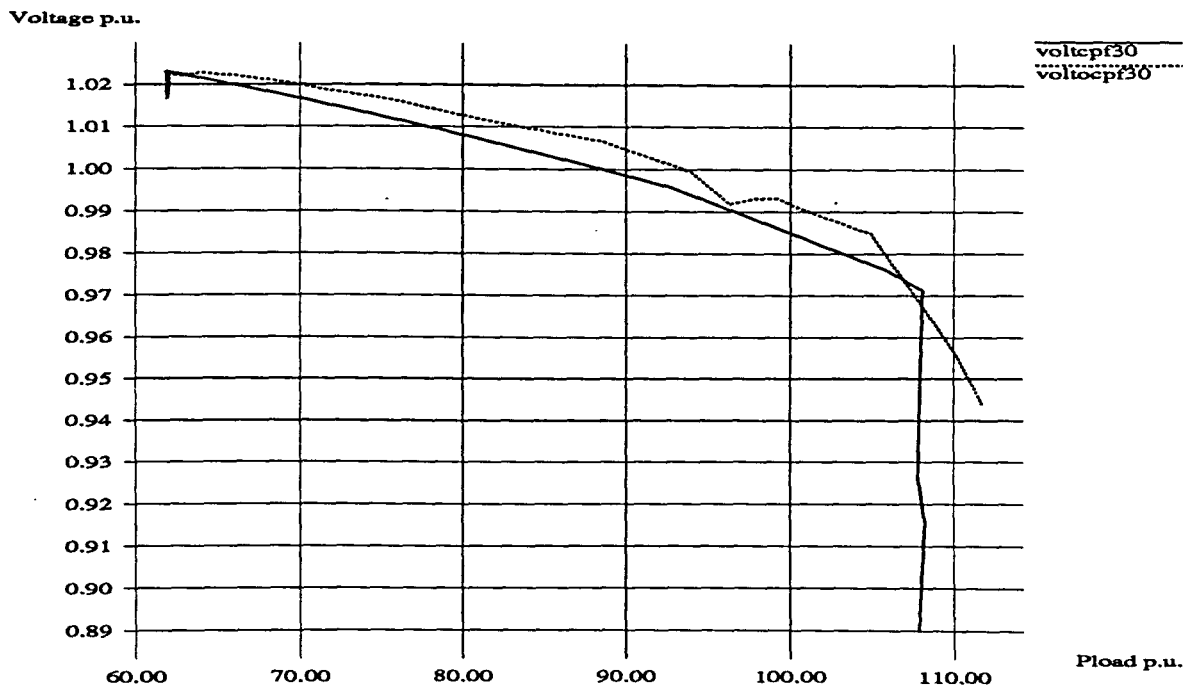


Figure 5.5: Comparison of the voltage at bus 24 for the CPF and the OCPF in 30-bus test system

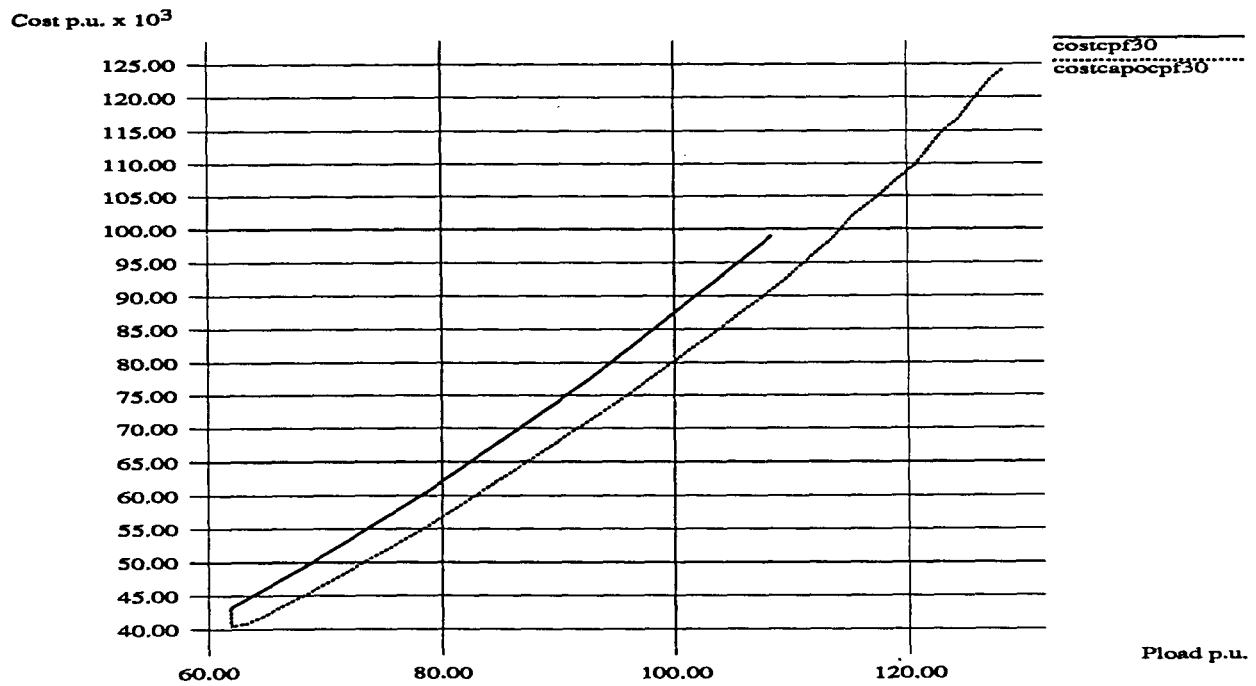


Figure 5.6: Comparison of the cost for the CPF and the CAPOCPF for 30-bus test system

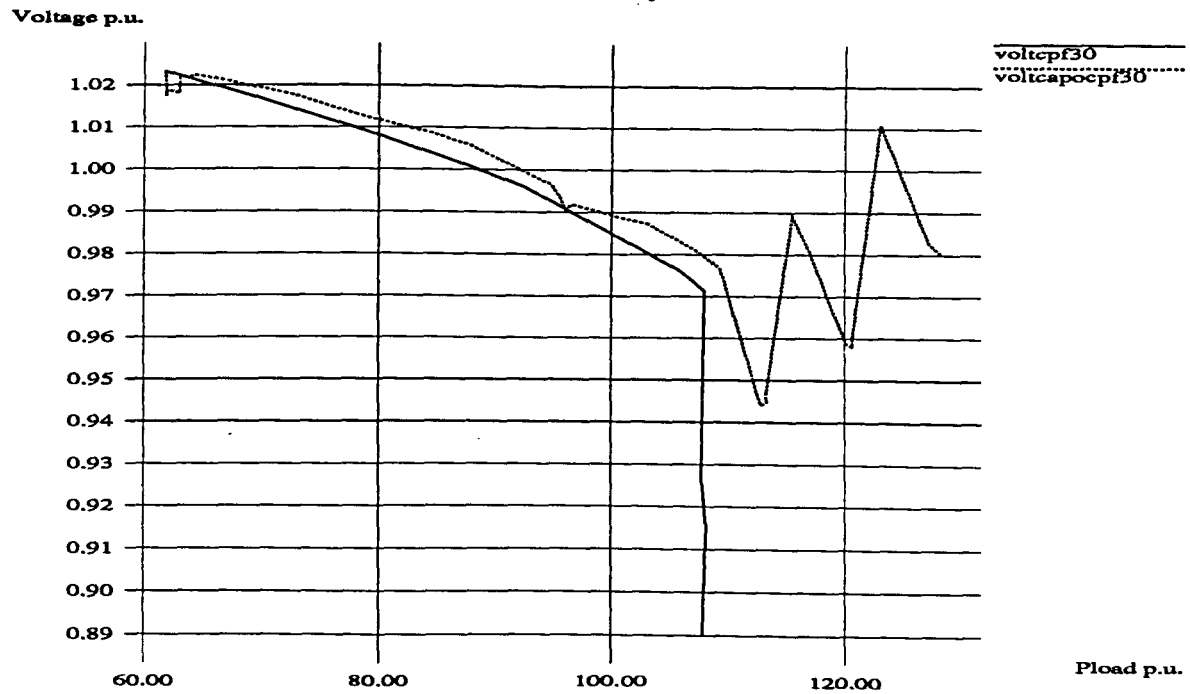


Figure 5.7: Comparison of the voltage at bus 24 for the CPF and the CAPOCPF in 30-bus test system

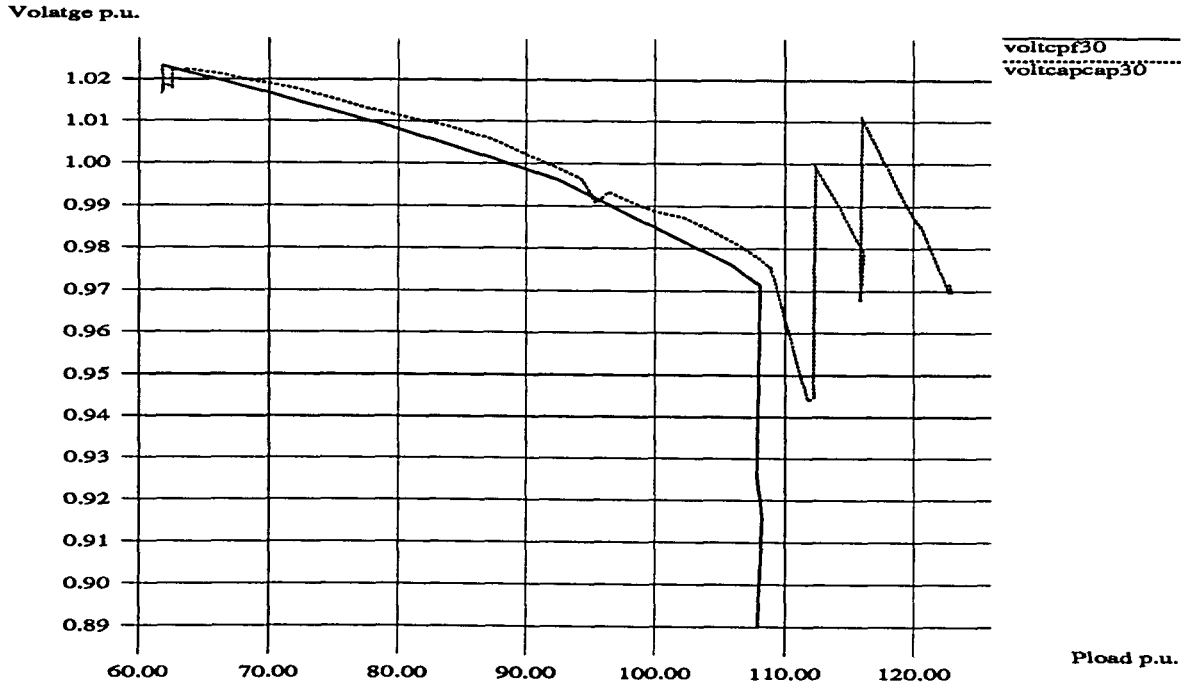


Figure 5.8: Comparison of the voltage at bus 24 for the CPF and the CAPOCPF in 30-bus test system with shunt reactors injected at the same load level

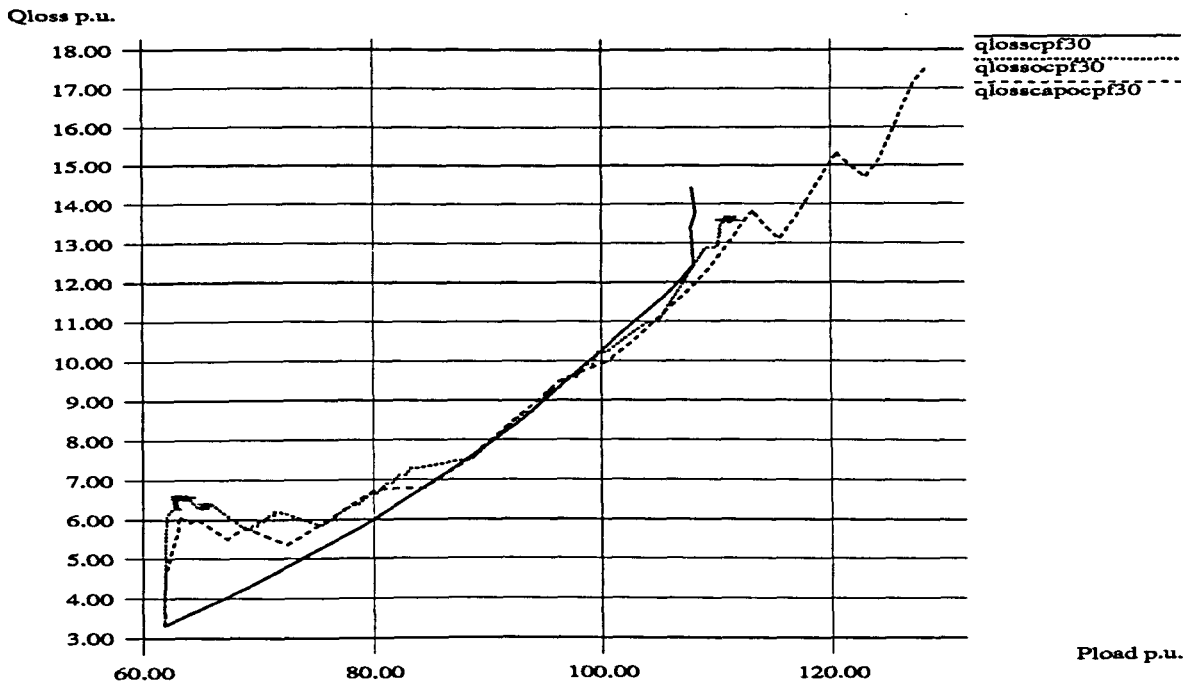


Figure 5.9: Comparison of the reactive losses for the CPF, OCPF, and CAPOCPF in 30-bus test system

162 reduced Iowa system: This reduced model of an actual Iowa power system is generally used for transient stability studies at Iowa State University. This model has now become the IEEE test system for stability studies. There are a total of 17 generators (PV buses) and 144 PQ buses in the system.

Figure 5.10 compares the total cost of generation for the CPF and the OCPF (without reactive power injection). It illustrates how the generation cost decreases during optimal tracking. The cost decreases greatly in the first few steps, but later the change slows and is even reversed. The slower rate of decrease in cost in the next few steps can be explained by the generation being increased in optimal direction corresponding to the load increase.

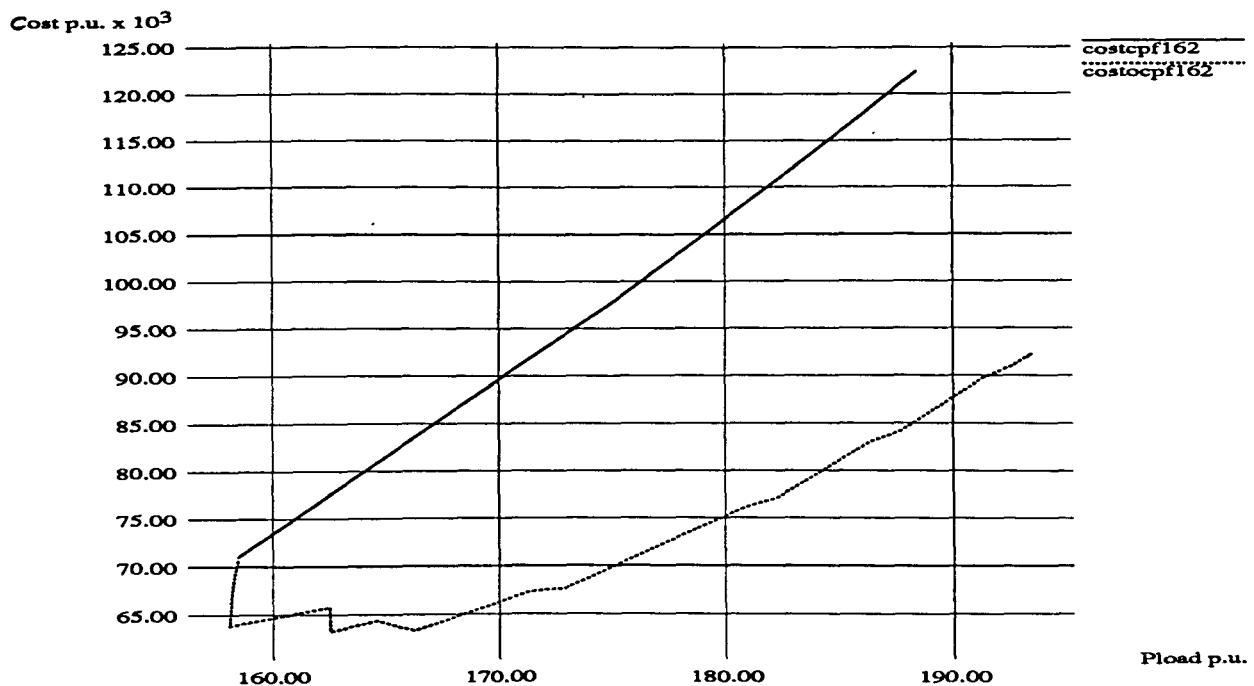


Figure 5.10: Comparison of the cost for the CPF and the OCPF for 162-bus test system

During the CPF run, bus 61 is observed to be one of the five most critical buses in this system. The voltage at bus 61 is used to compare the voltage profile for the CPF and the OCPF (without reactive power injection) in Figure 5.11. The CPF as well as the OCPF curves have been traced in this Figure up to the critical point. If 0.95 p.u. is considered to be the minimum acceptable limit for load voltages, then in the CPF total load capability of the system is 16,200 MW and in the OCPF, it is 17,700 MW.

Figure 5.12 compares the total cost of generation for the CPF and the CAPOCPF (the OCPF with shunt reactive power injection). The cost of additional shunt reactors installed at various load buses is not considered in the total cost of generation. The cost of generation for the CAPOCPF is always lower than the cost obtained in the CPF for a continuous increase in load.

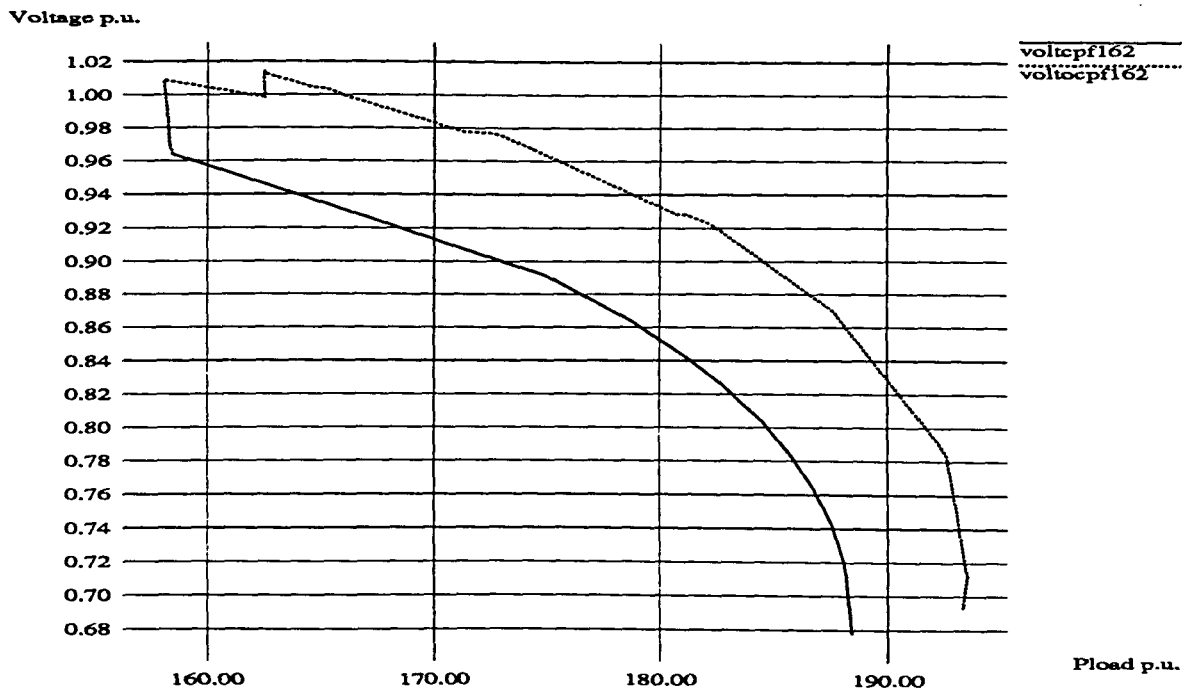


Figure 5.11: Comparison of the voltage at bus 61 for the CPF and the OCPF in 162-bus test system

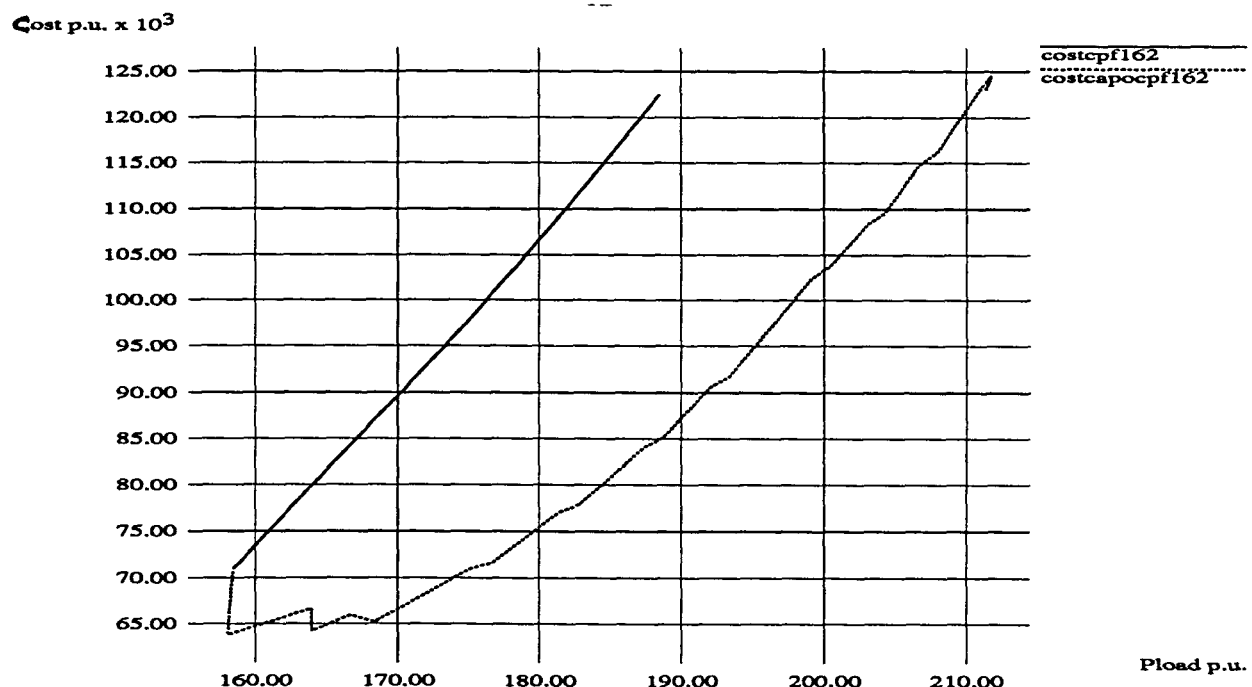


Figure 5.12: Comparison of the cost for the CPF and the CAPOCPF for 162-bus test system

Figure 5.13 compares the voltage profile obtained for the CPF and the CAPOCPF at load bus 61. The total increase in load from the base case up to the critical point is 3,000 MW for the highly stressed system in the CPF. The load voltages fall rapidly as the load is increased in the CPF. In the CAPOCPF efforts are made to control the load voltages once they fall below the acceptable limit via generator reactive power and reactive shunt compensation. The total power transfer capability is increased by 4,980 MW via the CAPOCPF. Figure 5.14 compares the reactive losses for the CPF, OCPF, and CAPOCPF. Reduced reactive losses are obtained with reactive power injection in CAPOCPF for this system. This results in from the fact that in CAPOCPF part of the local reactive load is supplied by shunt reactors. This leads to reduced effective reactive load and there by reduced reactive losses.

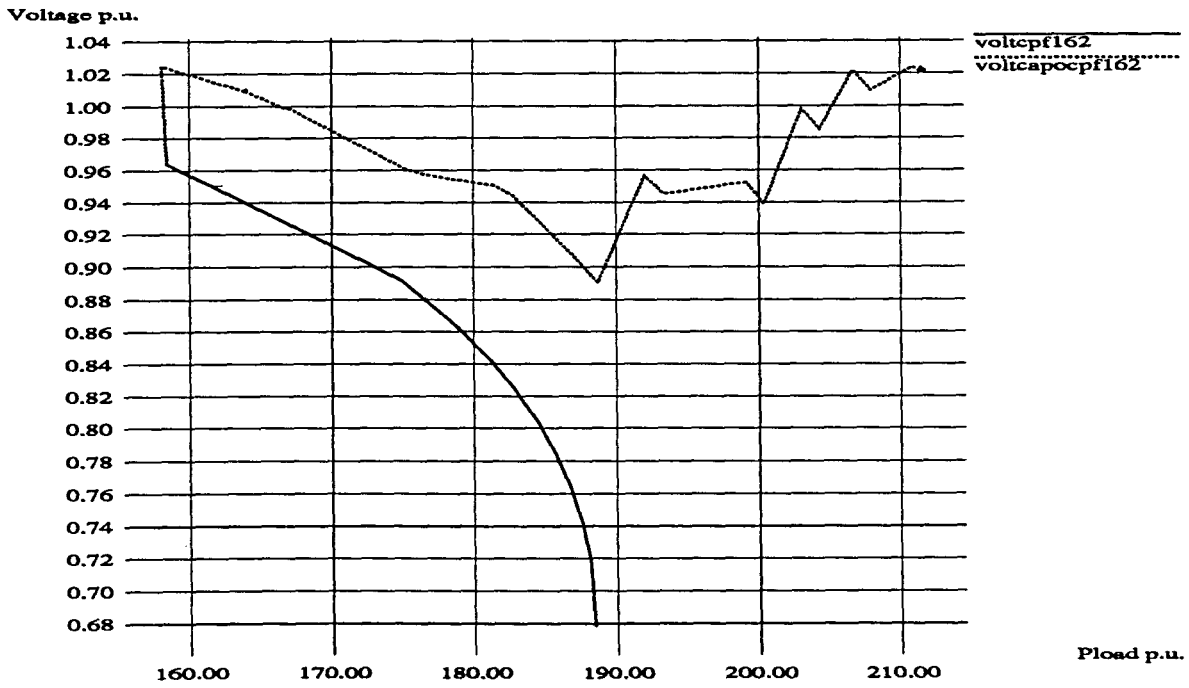


Figure 5.13: Comparison of the voltage at bus 61 for the CPF and the CAPOCPF in 162-bus test system

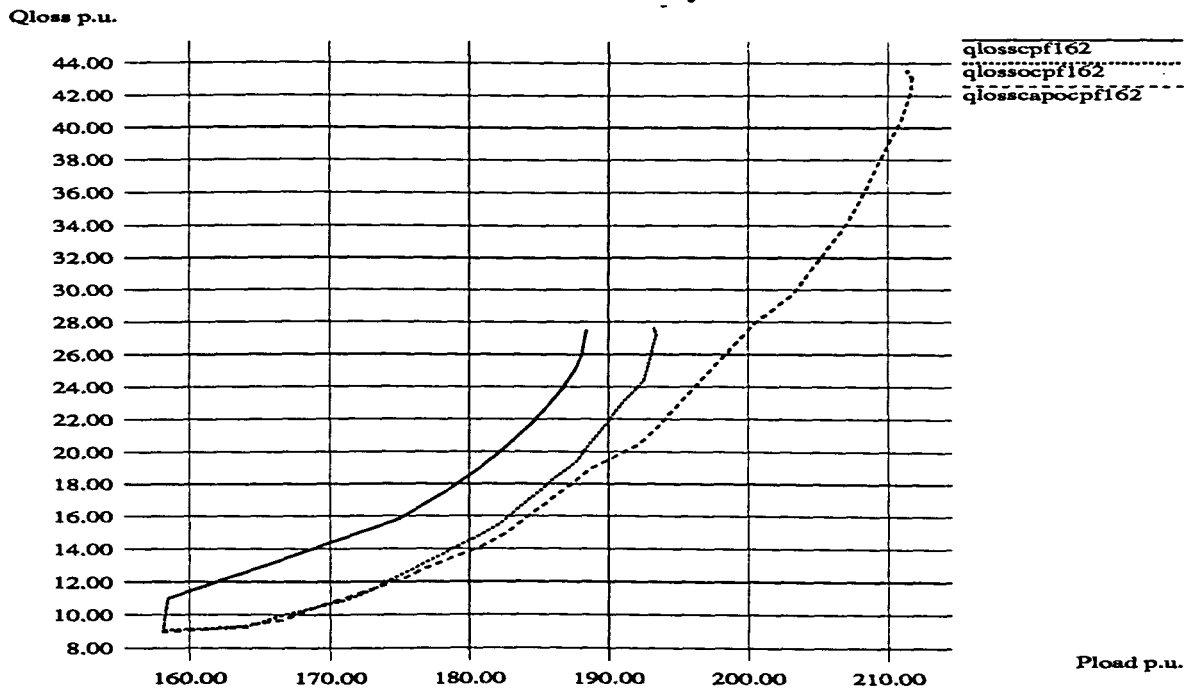


Figure 5.14: Comparison of the reactive losses for the CPF, OCPF, and CAPOCPF in 162-bus test system

Table 5.3: The CPF and the OCPF results for the 162-bus system

Method	Maximum system real power transfer in p.u.
CPF	162.0
OCPF without reactive power injection	177.0
OCPF with reactive power injection	211.8

Table 5.3 gives the transfer capability information for the CPF, OCPF, and CAPOCPF for this system.

1500 system power system network: Figure 5.15 compares the total cost of generation for the CPF and the OCPF. The total increase in load from the base case before the voltage collapse occurs is approximately 4,520 MW for this highly stressed network. Reduced cost of generation is obtained for a continuous increase in load via the OCPF algorithm.

Figure 5.16 compares the voltage profile at a bus for this system for the CPF and the OCPF. During the CPF run, bus 409 is observed to be the most critical bus for this system near the critical point. The voltage at bus 409 is used to compare the voltage profile for the CPF and the OCPF (without reactive power injection). If 0.95 p.u. is considered to be the minimum acceptable limit for load voltages, then in the CPF total load capability of the system is 74,520 MW and in the OCPF, it is 76,520 MW.

Figure 5.17 compares the total cost of generation for the CPF and the CAPOCPF (the OCPF with shunt reactive power injection). The cost of additional shunt reactors installed at various load buses is not considered in the total cost of generation. The cost of generation for the CAPOCPF is always lower than the cost obtained in the CPF for a continuous increase in load.

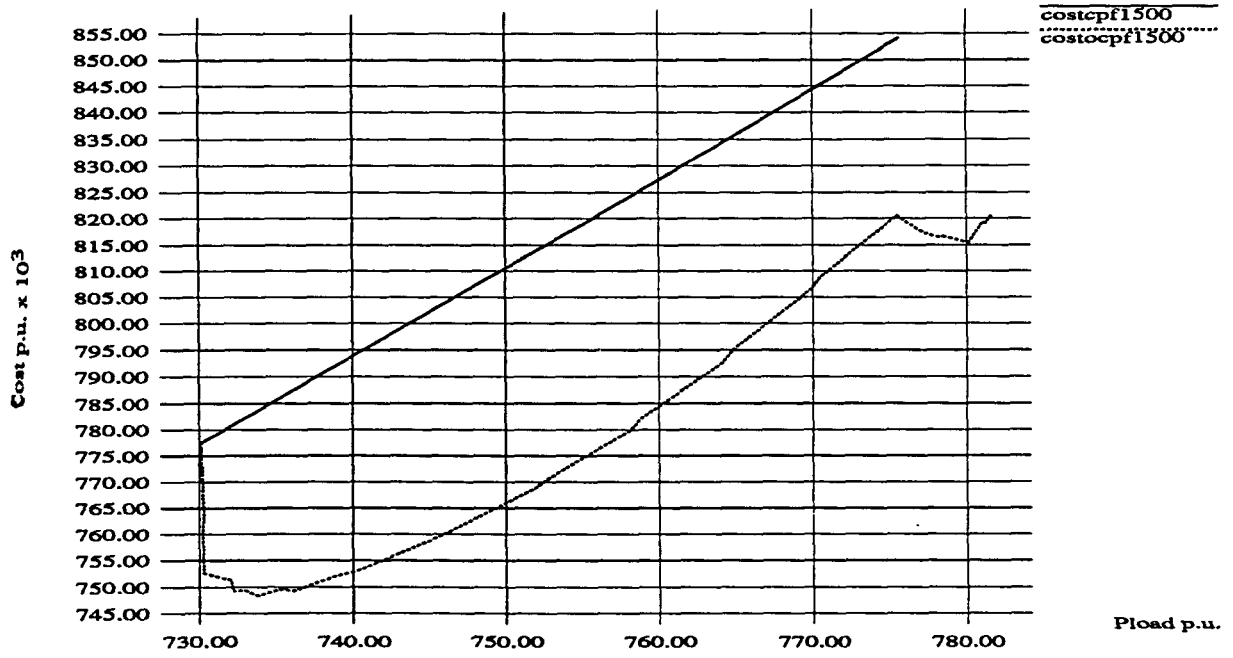


Figure 5.15: Comparison of the cost for the CPF and the OCPF for 1500-bus system

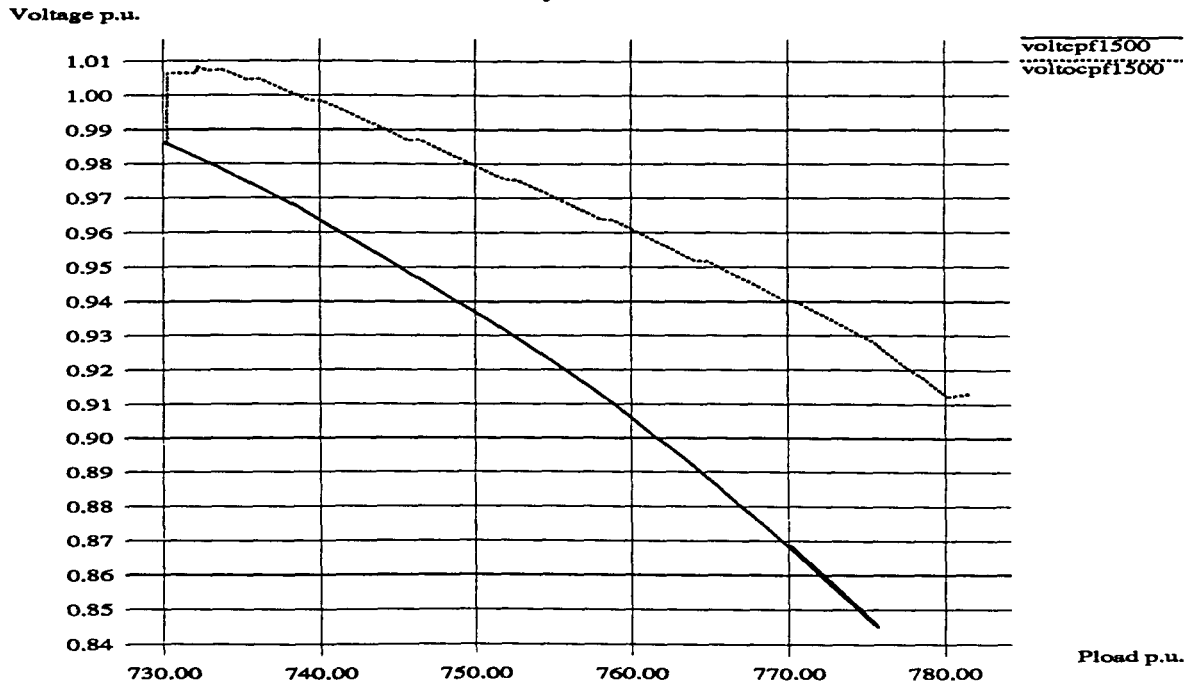


Figure 5.16: Comparison of the voltage at bus 409 for the CPF and the OCPF in 1500-bus system

Figure 5.18 compares the voltage profile obtained for the CPF and the CAPOCPF at load bus 409. The load voltages fall rapidly as load is increased in the CPF. In the CAPOCPF efforts are made to control the load voltages, once they fall below the acceptable limit via generator reactive power and reactive shunt compensation. Total power transfer capability is increased by 3,770 MW via CAPOCPF for this system. Table 5.4 compares the transfer capability of network for the CPF and the OCPF. Figure 5.19 compares the reactive losses for the CPF, OCPF, and CAPOCPF for this network and illustrates the reduced reactive losses obtained with reactive power injection.

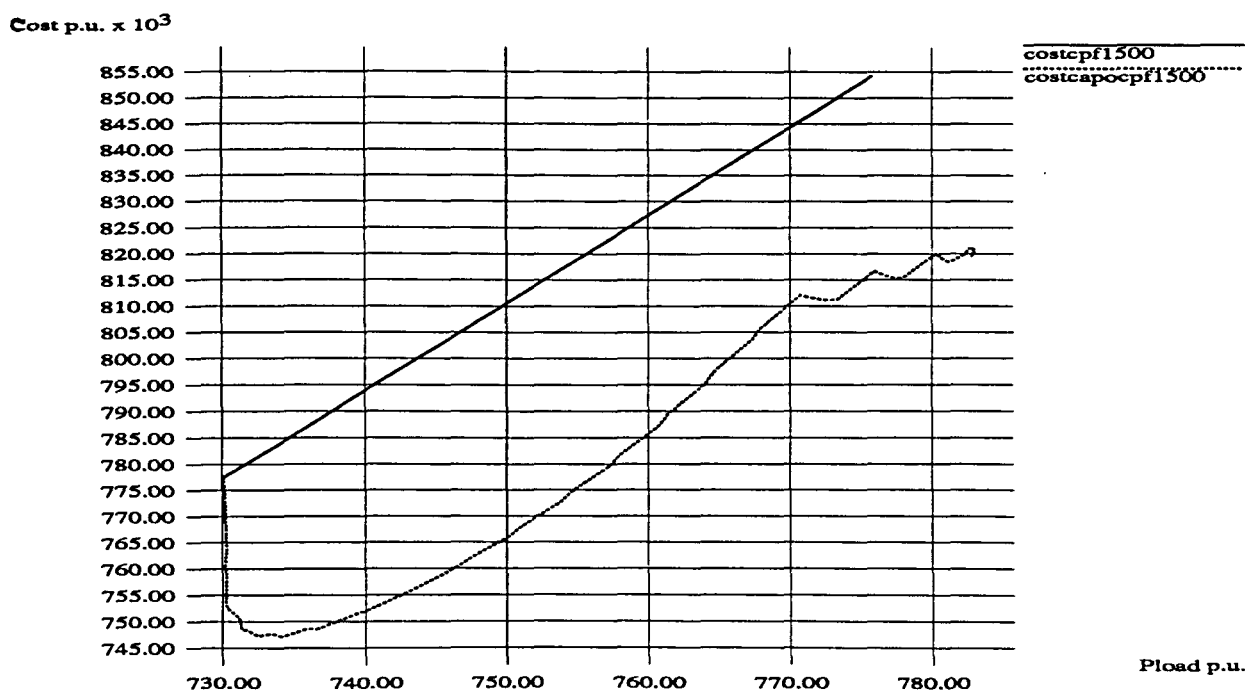


Figure 5.17: Comparison of the cost for the CPF and the CAPOCPF for 1500-bus system

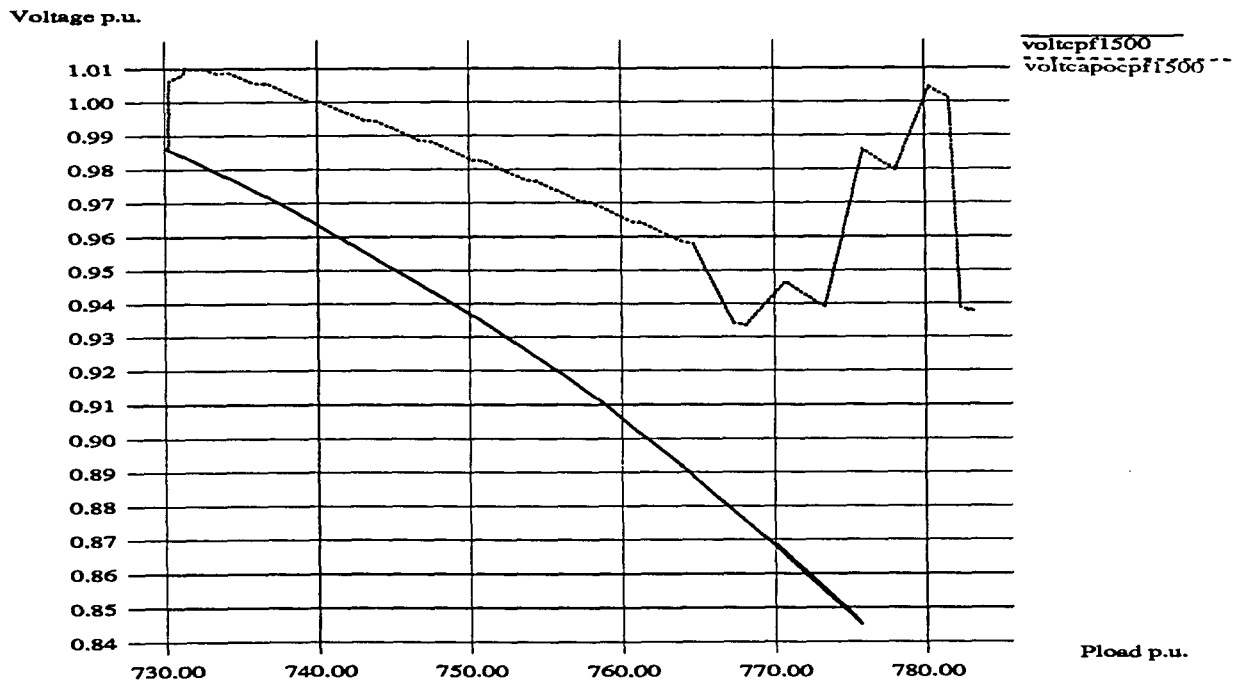


Figure 5.18: Comparison of the voltage at bus 409 for the CPF and the CAPOCPF in 1500-bus system

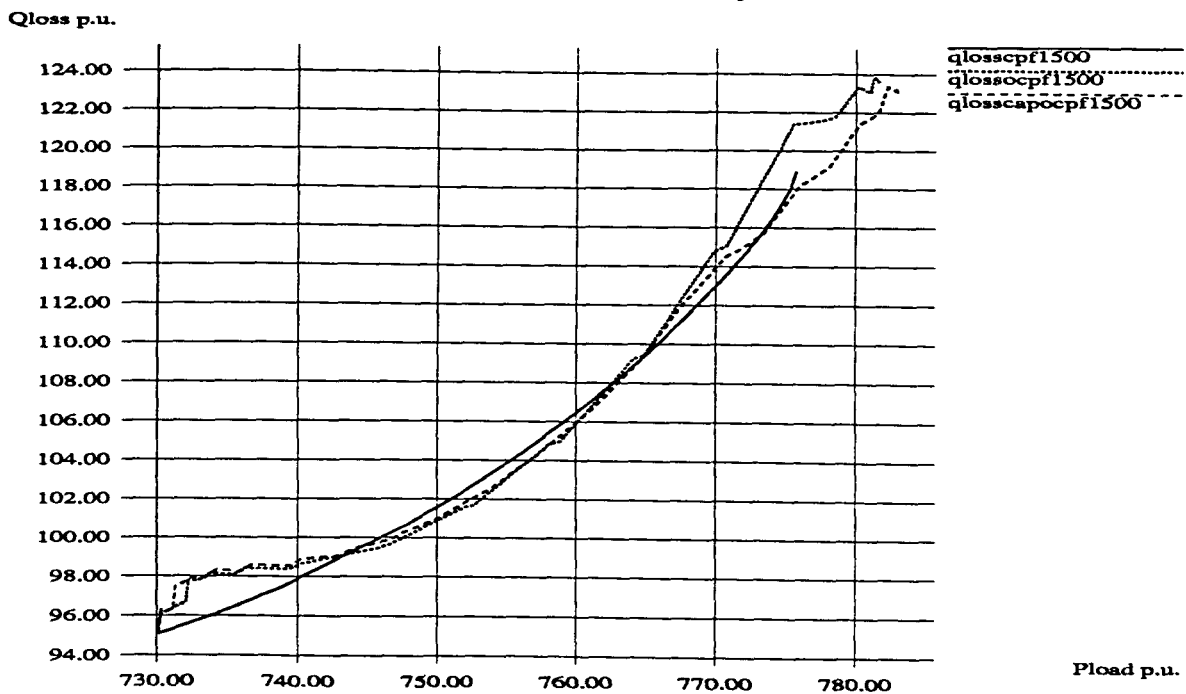


Figure 5.19: Comparison of the reactive losses for the CPF, OCPF, and CAPOCPF in 1500-bus test system

Table 5.4: The CPF and the OCPF results for the 1500-bus system

Method	System real power transfer in p.u.
CPF	745.2
OCPF without reactive power injection	765.2
OCPF with reactive power injection	782.9

Table 5.5 gives the value of capacitive and inductive reactors that are installed on the load buses in the CAPOCPF (OCPF with shunt reactive power injection) run to control the load voltages for the three system networks.

Table 5.6 shows the cpu time for the CPF, OCPF, and CAPOCPF on Sun Sparc stations for the above 3 power system network. The cpu time is not just for 1 optimal solution but for a series of optimal solutions up to the critical point is reached.

Table 5.5: Values of reactive sources installed at load buses

Type of system	Total value of capacitive sources installed p.u.	Total value of inductive sources installed p.u.
30-bus	10.89	1.82
162-bus	40.36	24.20
1500-bus	27.96	19.55

Table 5.6: Compares the execution time for the CPF, OCPF, and CAPOCPF

Type of system	CPF cpu time (s)	OCPF cpu time (s)	CAPOCPF cpu time (s)
30-bus	2.4	14.9	29.7
162-bus	12.9	183.3	343.3
1500-bus	1,444.8	5,131.0	8,348.0

6. CONCLUSIONS AND SUGGESTIONS FOR FUTURE WORK

6.1 Conclusions

System Planners and operators are seeking means to deal effectively with the voltage stability problem. They require analytical tools that are capable of

- Quantifying accurately the voltage stability margins
- Predicting voltage collapse in complex networks
- Defining power transfer limit
- Identifying voltage weak points and areas susceptible to voltage instability
- Determining critical voltage levels and contingencies
- Identifying key contributing factors and sensitivities affecting voltage instability

The CPF, with the different versions developed at Iowa State University, serves a portion of the needs of the power industry and has been used successfully to study the phenomenon of voltage instability in a group of complex networks. The CPF starts at a known power flow solution and then, via predictor and corrector schemes traces the solution curve until a critical point is reached. The CPF avoids the ill-conditioning of the Jacobian by using a well-conditioned augmented Jacobian.

This research attempts to use the present CPF algorithm and couple it with an OPF technique to develop the OCPF. The resulting OCPF provides a

new solution methodology for the optimal power flow problem for a continuous increase in load via a locally parametrized continuation method. This new methodology is flexible enough to use in calculating the sensitivities as proposed [40] and can be used to calculate the change in cost as the parameters are varied. With the OCPF, the cost of generation is minimized and voltages are maintained for a series of power flow solutions. In the OCPF, available reactive power is properly used and voltage collapse is delayed in terms of total active power transfer, even without injecting any reactive sources.

The calculation of an optimal solution near the critical point may be ill-conditioned. The proposed method avoids the ill conditioning by using the well-conditioned augmented Jacobian during the optimal corrector iterations. This OCPF methodology seems to work rapidly as the Jacobian is not updated continuously in the corrector iterations.

The OCPF methodology seems to be simple and flexible and has been found to work well when applied to real systems as large as 1,500 buses.

6.2 Suggestions for Future Work

This research focussed basically on the development of an OCPF algorithm to trace the optima of power flow solutions for a continuous increase in load via continuation method. Although the basic development is complete, many enhancements could be added and many features may be further investigated. These include:

- In the OCPF, the objective function used is the minimization of total cost of generation subjected to equality and inequality constraints. The cost of any

additional reactive sources installed at various load buses is not taken into account. Optimizing the cost of generation does not result in the reduced transmission losses as observed for the 3 test cases. However, once the real powers are scheduled, the voltages and reactive powers can be scheduled to reduce the transmission losses. Implementation of goal programming in the OCPF is necessary in the future to study the other available objective function simultaneously and to determine the affect of objective functions on each other.

- In the future, the Newton OPF technique is needed to be implemented in the OCPF to compare the gradient-based OCPF formulation in terms of speed and robustness.
- The inclusion of phase shift transformers in the CPF should be explored to achieve maximum real power transfer.
- Ways that could decrease the cpu time required to execute the OCPF should be investigated.
- In the 1993 IEEE winter power meeting, the voltage stability working group committee listed the following techniques to mitigate the voltage stability problems:

Must run generator: operate less economical generators to change the power flows and, thus, reduce the reactive demand when construction of new lines is delayed.

Series capacitors: use series capacitors to effectively shorten the electrical length of line and thereby reduce the reactive losses. As a result,

more reactive power can be delivered to the end of the line experiencing a reactive shortage.

Shunt capacitors: Supply the reactive power using shunt capacitors locally to reduce the reactive consumption across lines.

Load shedding: Use load shedding to reduce the reactive demand in avoiding voltage collapse.

Lower power factor generators: In areas where new generation is close to a reactive shortage or where the demand of large reactive reserve is occasional, low power factor generators may be helpful in avoiding voltage collapse.

Generator reactive overload capability: Use a generator's overload capability and exciters to delay voltage collapse until operators can vary the dispatch to reduce the reactive power.

A systematic approach that can utilize the above techniques in planning and operation does not exist. A detailed study is required to determine the most economic and effective means of mitigating the voltage collapse. Implementation of these schemes can be explored in the CPF. Use of FACT (Flexible A.C. Transmission) devices in the CPF is under investigation.

BIBLIOGRAPHY

- [1] Venikov, V. A., V. I. Store, V. I. Idelchick, and V. I. Tarasov. "Estimation of Power System Steady-State Stability in Load Flow Calculations," *IEEE Transactions on Power Apparatus and Systems*, Vol. PAS- 94, No. 3 (May/June 1975): pp. 1034-1041.
- [2] Ajarapu, V. "Identification of Steady State Voltage Stability in Power Systems," *Proceedings of IASTED International Conference on High Technology in Power Industry*, March 1st 1988.
- [3] Ajarapu, V. and C. Christy. "The Continuation Power Flow: A Tool for Steady - State Voltage Stability Analysis," *IEEE Transactions on Power Systems*, Vol. 7, No. 1 (Feb. 1992): pp. 416-423.
- [4] Tamura, Y., H. Mori and S. Iwamoto. "Relationship Between Voltage Instability and Multiple Load Flow Solutions in Electric Power Systems," *IEEE Transactions on PAS*, Vol. PAS-102, No. 5 (May 1983): pp. 1115-1125.
- [5] Alvarado, F. L. and T. H. Jung. "Direct Detection of Voltage Collapse Conditions," *Proceedings: Bulk Power System Voltage Phenomena Voltage Stability and Security*, Jan. 1989.
- [6] Tiranuchit, A. and R. J. Thomas. "A Posturing Strategy Against Voltage Instabilities in Electric Power Systems," *IEEE Transactions on Power Systems*, Vol. 3, No. 1 (Feb. 1988): pp. 87-93.
- [7] Rheinboldt, W. C. and I. V. Burkhardt. "A Locally Parametrized Continuation Process," *ACM Transactions on Mathematical Software*, Vol. 9, No. 2 (June 1983): pp. 215-2335.
- [8] Seydel, R. *From Equilibrium to Chaos*, Elsevier, New York, 1988.

- [9] Ajarapu, V. and S. Battula. "Sensitivity Based Continuation Power-Flow, " *Proceedings of 24th Annual North American Power Symposium*, Nevada, Oct. 1992.
- [10] Ajarapu, V. and C. Christy. "The Application of Locally Parametrized Continuation Technique to the Study of Steady-State Voltage Stability," *Proceedings of 21st Annual North American Power Symposium*, Rolla, Missouri, Oct. 1989.
- [11] Ajarapu, V., Ping Lin Lau, and S. Battula. " An Optimal Reactive Power Planning Strategy Against Voltage Collapse," *To be presented at IEEE Summer Power Meeting*, Vancouver, July 18-22 1993.
- [12] Christy, C. D. "Analysis of Steady State Voltage Stability in Large Scale Power Systems," M.S. Thesis, Iowa State University, Ames, IA, 1990.
- [13] Lau, P. L. "Optimal Continuation Power Flow," M.S. Thesis, Iowa State University, Ames, IA, 1991.
- [14] Battula, S. "Sensitivity Based Continuation Power Flow," M.S. Thesis, Iowa State University, Ames, IA, 1992.
- [15] Robert W. Roddy and Collin D. Christy. "Voltage Stability on the MAPP-MAIN Transmission Interface Wisconsin," *Proceedings of the EPRI / NERC Forum on Voltage Stability*, Colorado, Sep. 14-15 1992.
- [16] Flatabo, N., R. Ognedal, and T. Carlsen. "Voltage Stability Condition in a Power Transmission System Calculated by Sensitivity Methods," *IEEE/PES Summer Meeting 1989*, No. 89SM 771-1 PWRS, Long Beach, CA, July 9-14, 1989.
- [17] Sauer P. W. and M. A. Pai. "Power System Steady State Stability and the Load Flow Jacobian," *IEEE Transactions on Power Systems*, Vol. 5, No. 4 (Nov. 1990): pp. 1374-1383.

- [18] Kessel, P. and H. Glavistch. "Estimating the Voltage Stability of a Power System," *IEEE Transactions on Power Delivery*, Vol. PWRD-1, No. 3 (July 1986): pp. 346-354.
- [19] Obadina, O. O., G. F. Berg. "Determination Voltage Stability Limit in Multi Machine Systems," *IEEE/PES 1988 Winter Meeting*, No. 88 WM 194-3, New York, NY, 1988.
- [20] Cutsem, T. Van. "A Method to Compute Reactive Power Margins with Respect to Voltage collapse," *IEEE/PES Winter Meeting 1990*, No. 90WM 097-0 PWRs, Atlanta, GA, Feb. 4-8 1990.
- [21] Dobson, I. and Liming Lu. "New Methods For Computing a Closest Saddle Node Bifurcation and Worst Case Load Power Margins for Voltage Collapse," *IEEE Power Engineering Society Summer Meeting*, Seattle, WA, July 1992.
- [22] Iba, K., H. Suzuki, M. Egawa, and T. Watanabe. "Calculation of Critical Loading Condition with Nose Curve Using Homotopy Continuation Method," *IEEE Transactions on PWRs*, Vol. 6, No. 2 (May 1991): pp. 584-593.
- [23] Lof, P. A., T. Smed, G. Anderson, and D. J. Hill. "Fast Calculation of a Voltage Stability Index," *IEEE/PES Winter Meeting 1991*, No. 91 WM 203-0 PWRs, New York, NY, Feb. 3-7 1991.
- [24] Lof P. A., G. Anderson, and D. J. Hill. "Voltage Stability Indices for Stressed Power Systems," *IEEE/PES Winter Meeting 1992*, No. 92 WM 101-6 PWRs, New York, NY, Jan. 26-30 1992.
- [25] Galiana, F. D., Fahmideh Vojdani, A. Hunealt, and M. Juman. "Optimal Power System Dispatch Through the Continuation Method: Variation of Functional Inequality Limits," *Proceedings of the IEEE*

International Symposium on Circuits and Systems, California, May 1983.

- [26] Ponrajah, R. A. and F. D. Galiana. "The Minimum Cost Optimal Power-Flow Problem Solver Via the Restart Homotopy Continuation Method," *IEEE/PES 1988 Winter Meeting*, No. 88WM 1992, New York, NY, 1988.
- [27] Huneault, M. and F. D. Galiana. "An Investigation of the Solution to the Optimal Power-Flow Incorporating' Continuation Methods," *IEEE/PES 1989 Summer Meeting*, No. 89SM 694-1, New York, NY, 1989.
- [28] Carpentier, J. "Contribution to the Economic Dispatch Problem," (in French), *Bulletin de la Direction des Etudes et Rechert Electricite de France*, No. 1, 1966.
- ✓ [29] Dommel, H. W. and W. F. Tinney. "Optimal Power Flow Solutions," *IEEE Transactions on PAS*, Vol. PAS-87, No. 10 (Oct. 1968): pp. 1866-1876.
- ✓ [30] Sun, D.I., B. Ashley, B. Brewer, A. Hughes, and W.F. Tinney. "Optimal Power Flow Solution by Newton Approach," *IEEE Transactions on PAS*, Vol. 103, No. 10 (Oct. 1984): pp. 2864-2880.
- [31] Rakowska, J., R. T. Haftka and L.T. Watson. "An Active Set Algorithm for Tracing Parametrized Optima," *Structural Optimization*, Springer-Verlag, New York, 1991.
- ✓ [32] Walter L. and J. Snyder. "Linear Programming Adapted for Optimal Power Flow," *Leeds & Northup Company, North, Wales, PA*, 1990.
- ✓ [33] Burchett R. C., H. H. Happ, and K. A. Wiragu. "Large Scale Optimal Power Flow," *IEEE Transactions on Power Apparatus and System*, Vol. 101, No. 10 (Oct. 1982): pp. 3722-3732.

- ✓ [34] Happ H. H. "Optimal Power Dispatch-A Comprehensive Survey," *IEEE Transactions on Power Apparatus and Systems*, Vol. PAS-96, No. 3 (May 1977): 841-854.
- [35] Sun D. I., K. D. Demaree, and B. Brewer. "Application and Adaptation of Optimal Power Flow," *ESCA Corporation*, Bellevue, Washington, 1990
- [36] Tinney W. F., J. M. Bright, K. D. Demaree, and B. A. Hughes. "Some Deficiencies in Optimal Power Flow," *IEEE Transactions on Power Systems*, Vol. 3, No. 2 (May 1988): pp. 676-683.
- [37] Huneault M. and F. D. Galiana. "A Survey of the Optimal Power Flow Literature," *IEEE Transactions on Power Systems*, Vol. 6, No. 2 (May 1991): pp. 762-770.
- [38] Monticelli A. and Wen-Hsiung E. Liu. "Adaptive Movement Penalty Method for the Newton Optimal Power Flow," *IEEE/PES Winter Meeting*, No. 90 WM 251-9 PWRS, Atlanta, GA, Feb. 1990.
- [39] Anwar D. "Application of Optimal Power Flow to Interchange Brokerage Transaction," M.S. Thesis, Iowa State University, Ames, IA, 1992.
- [40] Paul R. Gibrik, D. Shirmohammadi, S. Hao and C. L. Thomas. "Optimal Power Flow Sensitive Analysis," *IEEE/PES Winter Meeting*, No. WM 23-1 PWRS, Atlanta, GA, Feb 4-8 1990.
- [41] Venkataramana, A., J. Carr, and R. S. Ramshaw. "Optimal Reactive Power Allocation," *IEEE Transactions on Power Systems*, Vol. PWRS-2, No. 1 (Feb. 1987): pp. 138-144.
- [42] Hernando, D. "Optimum Number, Location, and Size of Shunt Capacitors in Radial Distribution Feeders, A Dynamic Programming

Approach," *Presented at the IEEE Winter Power Meeting, New York, NY, Jan. 29-Feb. 3, 1967.*

- [43] Chiang, H. D., J. C. Wang, O. Cockings, and H. D. Shin. "Optimal Capacitor Placements in Distribution Systems: Part 1: A New Formulation and the Overall Problem," *IEEE Transactions on Power Delivery*, Vol. 5, No. 2 (April 1989): pp. 634-641.
- [44] Luenberger, D.G. *Linear and Nonlinear Programming*, 2nd. ed. Addison-Wesley Publishing Co., Reading, Massachusetts, 1984.
- [45] Fletcher, R. *Practical Methods of Optimization*. John Wiley and Sons Inc., New York, 1987.
- [46] Stagg, G. L. *Computer-Aided Power System Analysis*. NJ: Prentice-Hall Inc., Englewood Cliffs, New Jersey, 1986.
- [47] Heydt, G. T. *Computer Analysis Methods for Power Systems*. Macmillian Publishing Co., New York, 1986.
- [48] Debs, A. S. *Modern Power Systems Control and Operation*, Debs, Georgia, 1991.
- [49] Stevenson, W. D. *Elements of Power System Analysis*, 4th ed., McGraw Hill Inc., New York, 1982.

ACKNOWLEDGEMENTS

I am deeply indebted to my major professor, Dr. Ajarapu, for providing support, guidance, and direction during my research work and in times of doubt. I would like to extend my gratitude both to the Electric Power Research Center for providing financial support during my graduate program and to the members of the power faculty under whom I took graduate courses. I also thank all my committee members for reviewing the thesis.

Finally I thank my family members for their help and encouragement.

APPENDIX A: FORMULATION OF POWER FLOW EQUATIONS IN CPF

Let μ represent the load parameter such that

$$0 \leq \mu \leq \mu_{\text{critical}}$$

Here $\mu = 0$ corresponds to the base load and μ_{critical} corresponds to the critical point. It is desired to incorporate μ into the following power flow equations:

$$0 = P_{Gi} - P_{Li} - P_{Ti}, P_{Ti} = \sum_{j=1}^n V_i V_j Y_{ij} \cos(\delta_i - \delta_j - \theta_{ij})$$

$$0 = Q_{Gi} - Q_{Li} - Q_{Ti}, Q_{Ti} = \sum_{j=1}^n V_i V_j Y_{ij} \sin(\delta_i - \delta_j - \theta_{ij})$$

Here i is index for the i th bus and the subscripts L, G, T denote load, generation, and injection, respectively. V_i and V_j represent the voltages at buses i and j and $Y_{ij} \angle \theta_{ij}$ is the $(i, j)^{\text{th}}$ element of Y bus.

Terms P_{Li} and Q_{Li} are modified to simulate the load change. Modification consists of breaking each term into two components. One component corresponds to the base load; the other corresponds to change in the load brought about by a change in the load parameter μ .

$$P_{Li} = P_{Lio} \times (1 + \mu \times \text{pmult}_i)$$

$$Q_{Li} = Q_{Lio} \times (1 + \mu \times \text{qmult}_i)$$

Here P_{Lio} , Q_{Lio} are original active and reactive load at bus i ; pmult_i , qmult_i represents the direction of the load increase. The active power generation is modified corresponding to increase in load by

$$P_{Gi} = P_{Gio} \times \left(1 + \frac{\text{total change in load}}{\text{total base load generation}}\right)$$

If these new expressions are substituted into the power flow equations, this results in

$$0 = P_{G_{i0}} \times \left(1 + \frac{\text{total change in load}}{\text{Total base load generation}}\right) - P_{L_{i0}} \times (1 + \mu \times \text{pmult}_i) - P_{T_i}$$

$$0 = Q_{G_{i0}} - Q_{L_{i0}} \times (1 + \mu \times \text{qmult}_i) - Q_{T_i}$$

The values of pmult_i and qmult_i can be uniquely specified for each bus in the system.

APPENDIX B: GRADIENT BASED OPF FORMULATION

In the basic load flow problem, given load demands at various load buses and generation levels at specified supply voltages are assumed. It is desired to obtain voltage profile, real and reactive flows on transmission lines, phase angles, line currents, line losses and other related steady state variables. The power flow equations are given by:

$$0 = P_{Gi} - P_{Li} - P_{Ti}, P_{Ti} = \sum_{j=1}^n V_i V_j Y_{ij} \cos(\delta_i - \delta_j - \theta_{ij})$$

$$0 = Q_{Gi} - Q_{Li} - Q_{Ti}, Q_{Ti} = \sum_{j=1}^n V_i V_j Y_{ij} \sin(\delta_i - \delta_j - \theta_{ij})$$
(B1)

The above nonlinear power flow equations are solved by the Newton Raphson iterative method.

$$\begin{bmatrix} H & N \\ J & L \end{bmatrix} \begin{bmatrix} \Delta\theta \\ \Delta v/v \end{bmatrix} = \begin{bmatrix} \Delta P \\ \Delta Q \end{bmatrix}$$

Here $\Delta\theta$ and $\Delta v/v$ are the vector of the voltage angle and the relative voltage magnitude correction. H, N, J, L are sub-matrices of the Jacobian matrix. ΔP and ΔQ are the vectors of the residuals given by:

$$\Delta P = P_{Gi} - P_{Li} - P_{Ti}$$

$$\Delta Q = Q_{Gi} - Q_{Li} - Q_{Ti}$$

$\Delta\theta$ and $\Delta v/v$ are calculated iteratively and substituted in Equation (B1) until the norm of $\Delta P, \Delta Q$ residuals obtained is sufficiently small.

$$H_{km} = \frac{\partial P_k(v, \theta)}{\partial \theta_m}, N_{km} = \frac{\partial P_k(v, \theta) \times v_m}{\partial v_m}, J_{km} = \frac{\partial Q_k(v, \theta)}{\partial \theta_m}, L_{km} = \frac{\partial Q_k(v, \theta) \times v_m}{\partial v_m}$$

Once the power flow equations are solved, the control parameters are changed in the optimal direction. The Lagrangian multipliers are calculated as

$$\begin{bmatrix} H & N \\ J & L \end{bmatrix} \begin{bmatrix} \lambda_P \\ \lambda_Q \end{bmatrix} = -z \begin{bmatrix} H_1 \\ N_1 \end{bmatrix} - \begin{bmatrix} \Sigma \partial \omega_j(\theta) / \partial \theta \\ \Sigma \partial \omega_j(v) \times v / \partial v \end{bmatrix}$$

ω_j are the penalty terms, λ_P and λ_Q are the Lagrangian multipliers corresponding to the real and reactive power equality constraints, and $z =$

$$\frac{\partial K_1}{\partial P_{G1}}$$

After the Lagrangian multipliers are calculated, the gradient vector with respect to all control parameters is computed. The components are as follows:

Generation control

$$\frac{df}{dPG_1} = \frac{\partial K_1}{\partial PG_1} + \Sigma \frac{\partial \omega_j(PG_1)}{\partial PG_1}$$

$$\frac{df}{dPG_i} = \frac{\partial K_i}{\partial PG_i} + \Sigma \frac{\partial \omega_j(PG_i)}{\partial PG_i} - \lambda_{P_i}$$

Generator voltage control

$$\frac{df}{dv_i} = \frac{1}{v_i} \left\{ \frac{\partial K_1}{\partial PG_i} \frac{\partial P_1}{\partial v_i} v_i + \sum_{\substack{m = \text{all nodes} \\ \text{including } i}} \lambda_{P_m} \frac{\partial P_m}{\partial v_i} + \sum_{\substack{m = PQ \text{ nodes} \\ \text{adjacent to } i}} \lambda_{Q_m} \frac{\partial Q_m}{\partial v_i} v_i \right\} + \Sigma \frac{\partial \omega_j(v_i)}{\partial v_i}$$

Once the gradient vector is obtained, the direction of search is obtained in negative direction of the gradient vector.

$$DS_i = \begin{cases} 0 & \text{if } \partial f/\partial u < 0 \text{ and } u_i = u_{i\max} \\ 0 & \text{if } \partial f/\partial u > 0 \text{ and } u_i = u_{i\min} \\ -\partial f/\partial u_i & \text{else} \end{cases}$$

where u is any control parameter. Control parameters are adjusted as

$$u_i = \begin{cases} u_{i\max} & \text{if } u_i - c_i * \partial f/\partial u_i > u_{i\max} \\ u_{i\min} & \text{if } u_i - c_i * \partial f/\partial u_i < u_{i\min} \\ u_i - c_i \partial f/\partial u_i & \text{else} \end{cases}$$

Here c is a scalar and represents the step size.